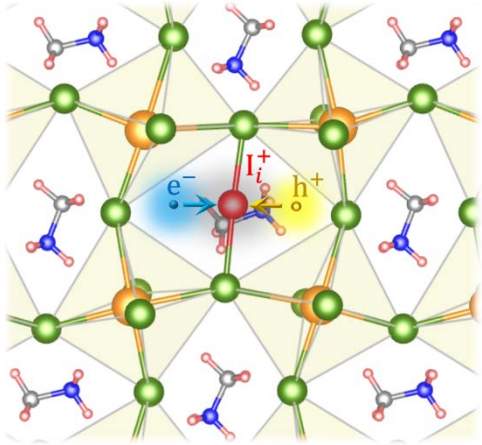

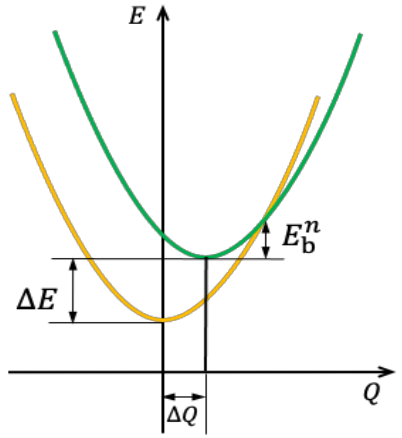

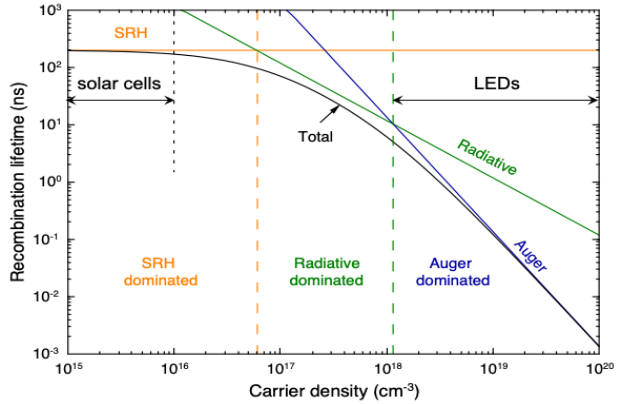

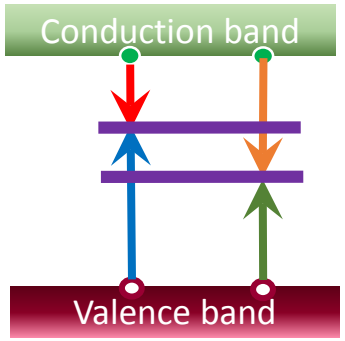

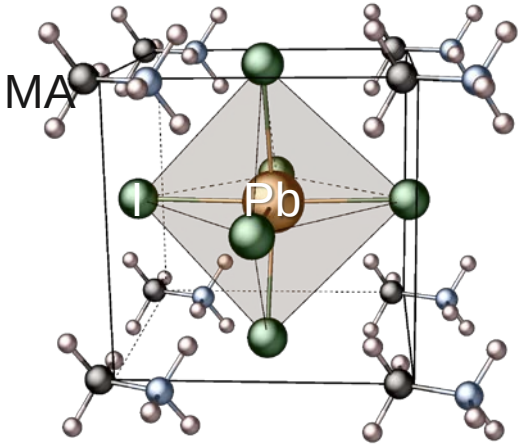

First-principles modeling of efficiency of halide perovskites

Chris G. Van de Walle

Materials Department, University of California, Santa Barbara

with

Xie Zhang

Beijing Computational Science Research Center

Mark Turiansky

Jimmy-Xuan Shen

ICOOPMA-EuroDIM 2022
Ghent, Belgium
July 3-8, 2022

Supported by DOE

UC SANTA BARBARA

Van de Walle Computational Materials Group

vandewalle.materials.ucsb.edu

First-principles calculations

Density functional theory, many-body perturbation theory

Oxides

- Transparent conductors
- Dielectrics
- Thermal barriers
- Complex oxides
- Power electronics

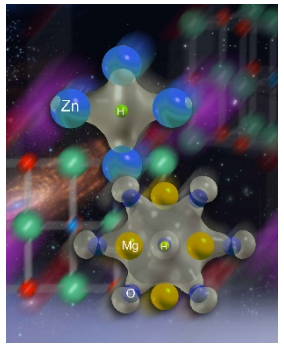

Nitrides

- Doping
- Surfaces
- Interfaces
- Efficiency, loss

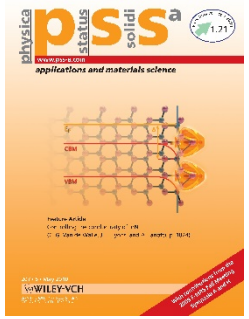

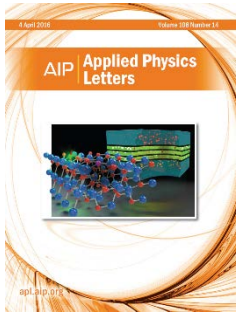

Quantum defects

- Qubits
- Single photon emitters
- Decoherence

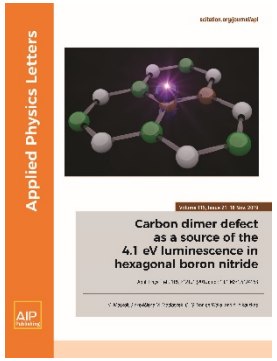

Hybrid perovskites

- Recombination mechanisms
- Defects
- Impurities
- Efficiency

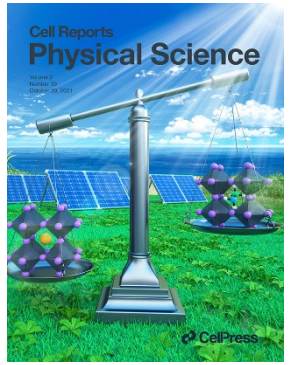

UC SANTA BARBARA

Halide perovskites

- Efficient optoelectronic materials
  - Solar cells, light emitting diodes (LEDs)

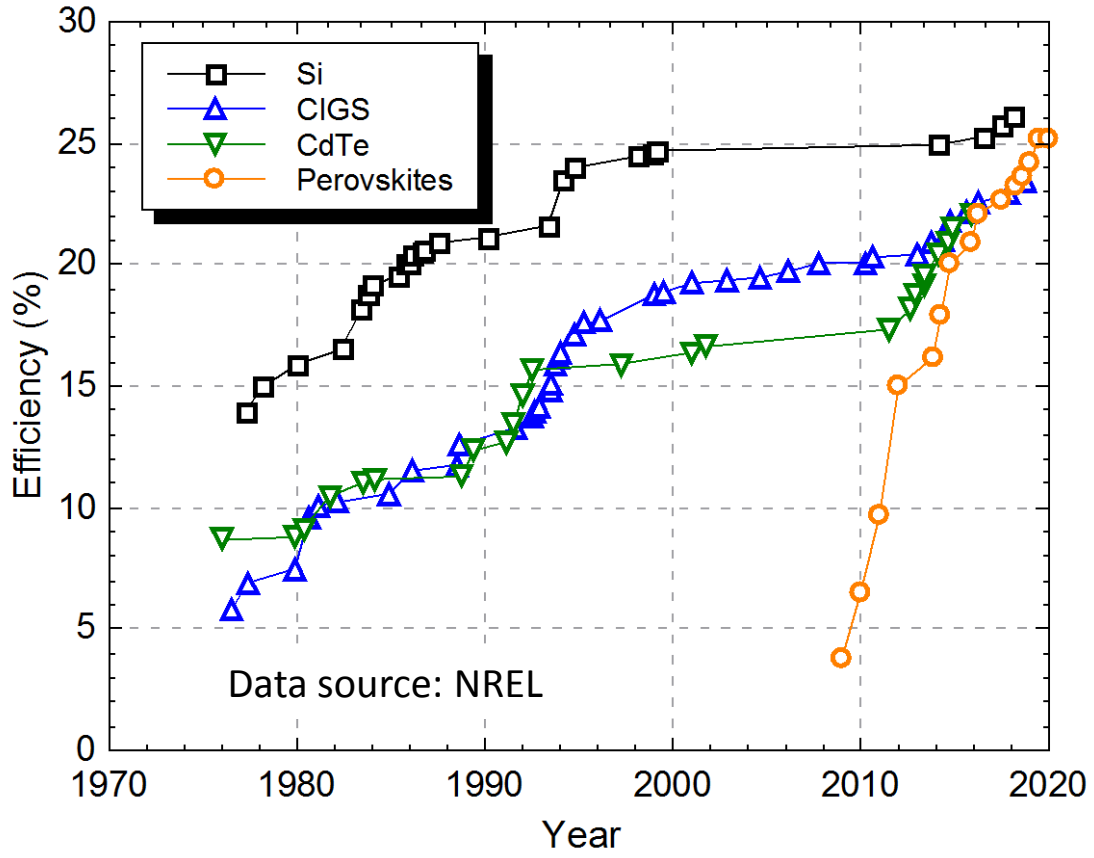

- Prototype: methylammonium lead iodide $MAPbI_3$
- General: ABX_3
  - A: Cs^+, MA^+, FA^+
  - B: Pb^{2+}, Sn^{2+}
  - X: I^-, Br^-, Cl^-…

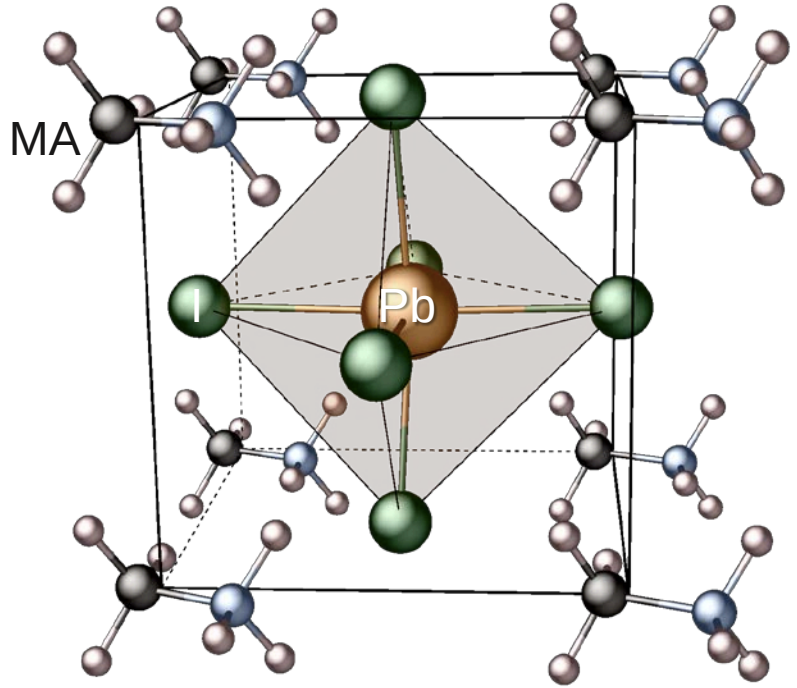

Recombination mechanisms

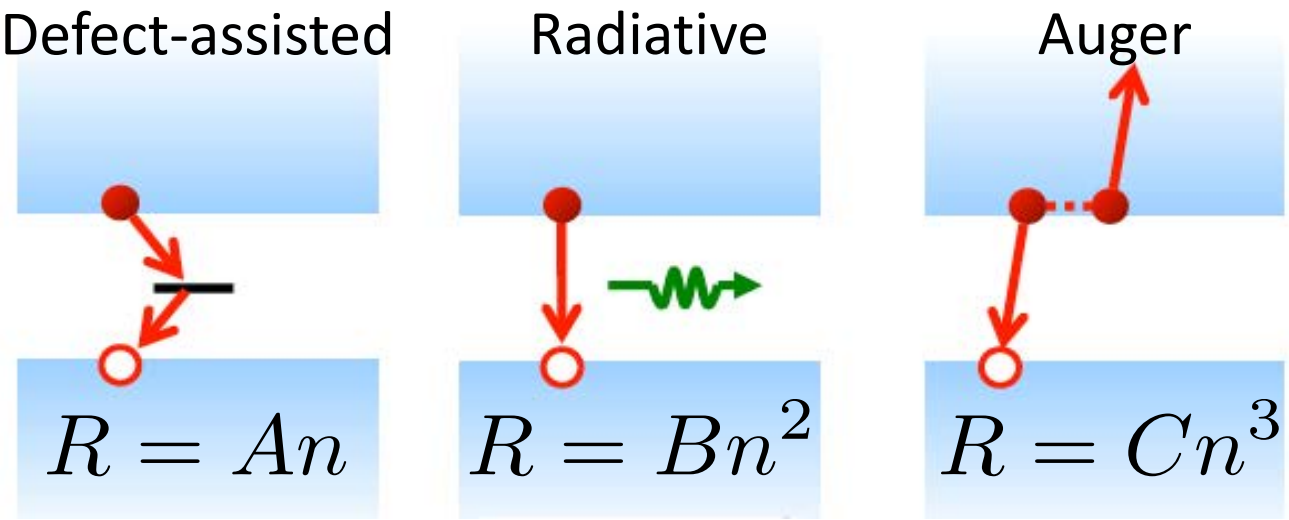

"Shockley-Read-Hall" (SRH)

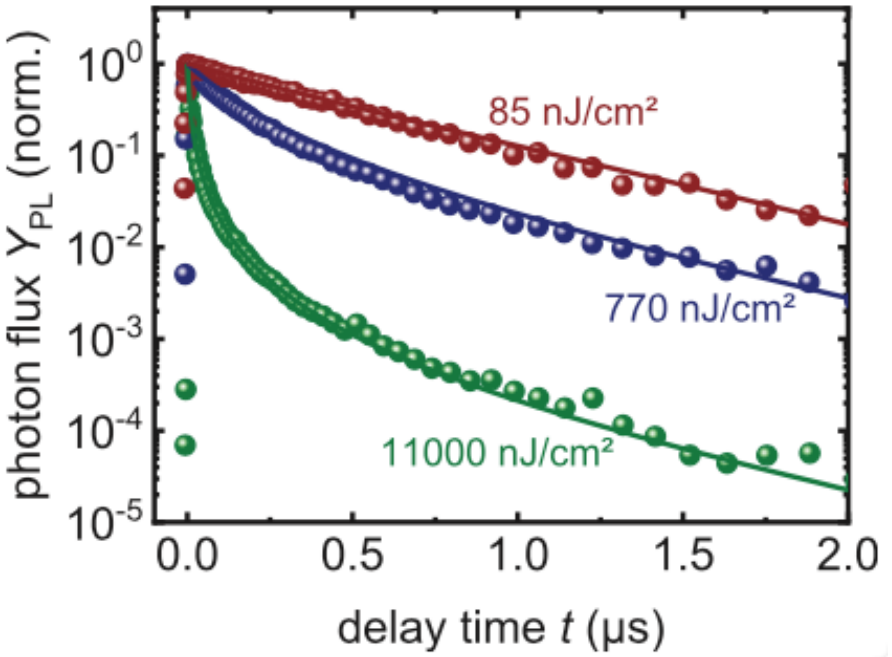

T. Kirchartz *et al.*,
Adv. Energy Mater. **10**, 1904134 (2020).

n: carrier density

Rate equation: $\frac{dn}{dt} = -An - Bn^2 - Cn^3$

Fitting to experimental data can introduce uncertainties, and does not elucidate fundamental mechanisms

Recombination in halide perovskites

First-principles studies of recombination rates

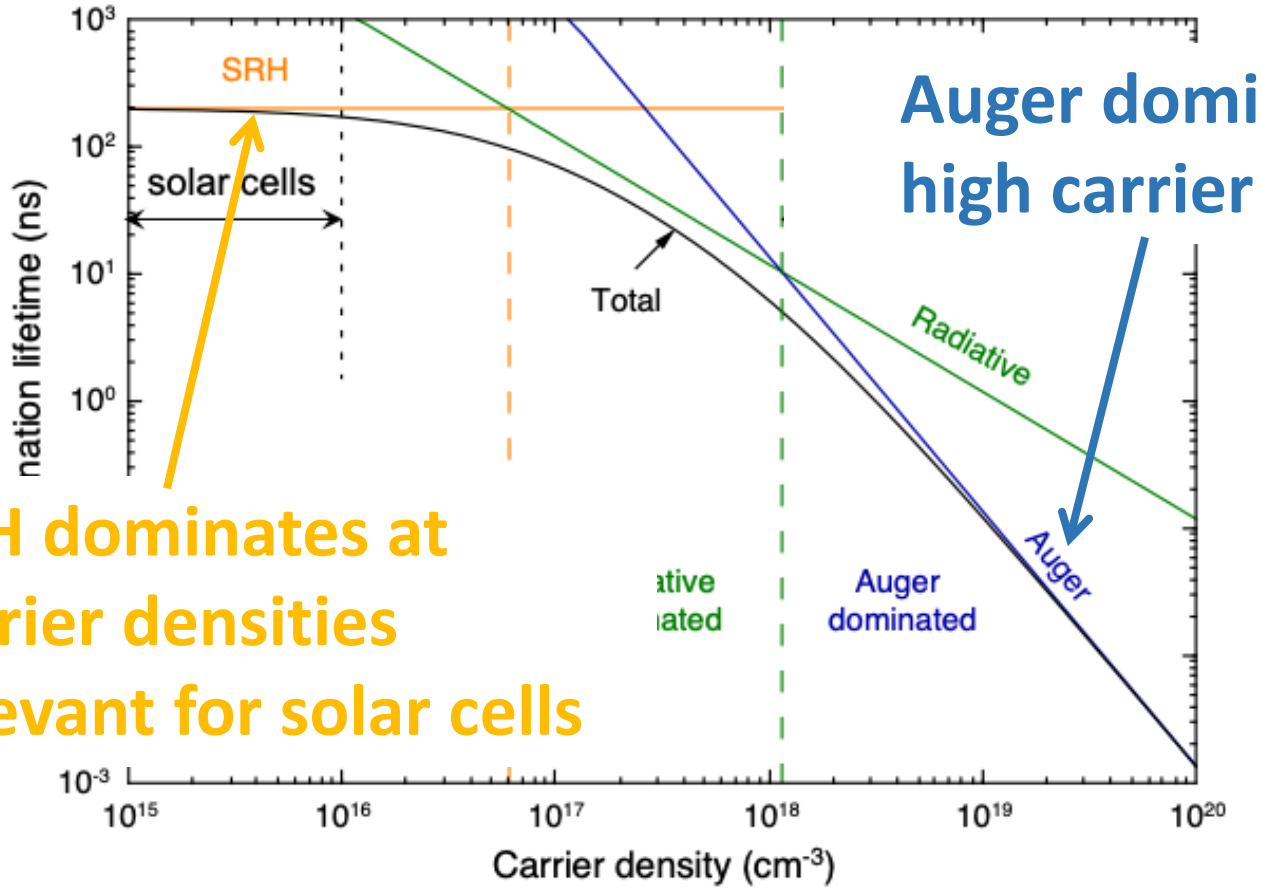

Auger dominates at high carrier densities

SRH dominates at carrier densities relevant for solar cells

X. Zhang *et al.*, Adv. Energy Mater. **10**, 1902830 (2020).

X. Zhang *et al.*, J. Phys. Chem. Lett. **9**, 2903 (2018).

X. Zhang *et al.*, ACS Energy Lett. **3**, 2329 (2018).

J.-X. Shen *et al.*, Adv. Energy Mater. **8**, 1801027 (2018).

Focus of this talk

- First-principles studies
  - Radiative recombination
  - Auger recombination
  - Defect-assisted
    Shockley-Read-Hall (SRH) recombination

❑ First-principles approach:

Density functional theory

- HSE hybrid functional

  J. Heyd *et al*., J. Chem. Phys. **118**, 8207 (2003).

- Vienna Ab-initio Simulation Package (VASP); Quantum Espresso

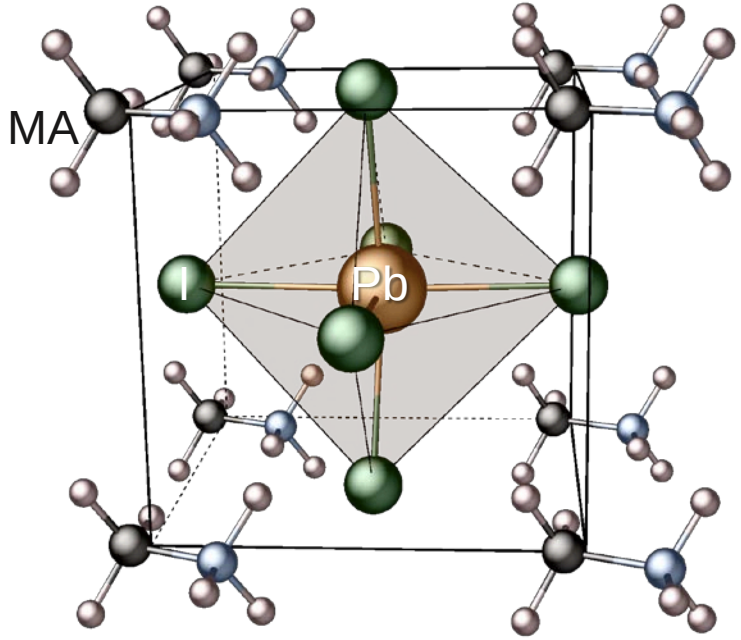

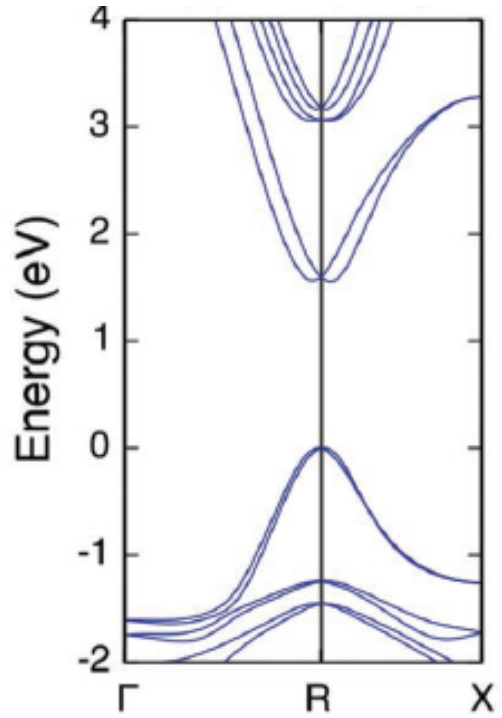

Slow radiative recombination?

Rashba spin-orbit coupling

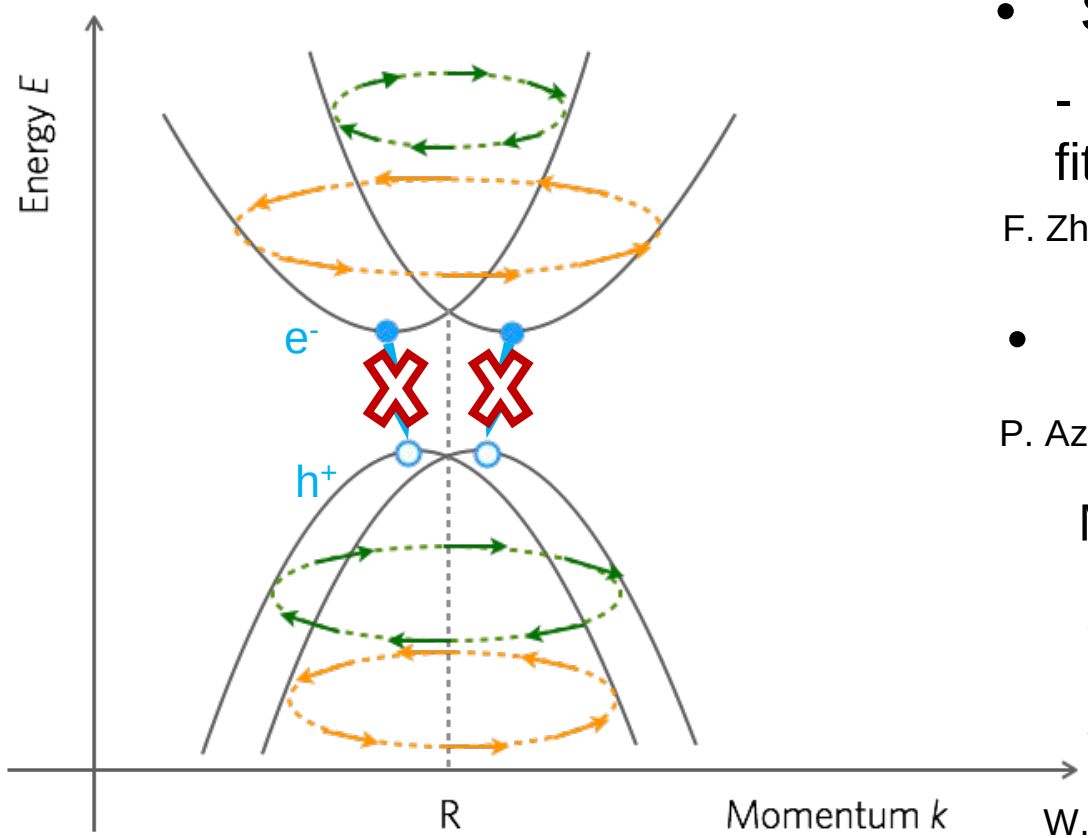

- Spin mismatch

  - Phenomenological model with fitted parameters

F. Zheng *et al*., Nano Lett. **15**, 7794 (2015).

- Momentum mismatch

P. Azarhoosh *et al*., APL Mater. **4**, 091501 (2016).

$MAPbI_3$: ~10^{-13} cm^3s^{-1}

GaAs: ~10^{-9} cm^3s^{-1}

Si: ~10^{-14} cm^3s^{-1}

W. Tress, Adv. Energy Mater. **7**, 1602358 (2017).

First-principles spin texture

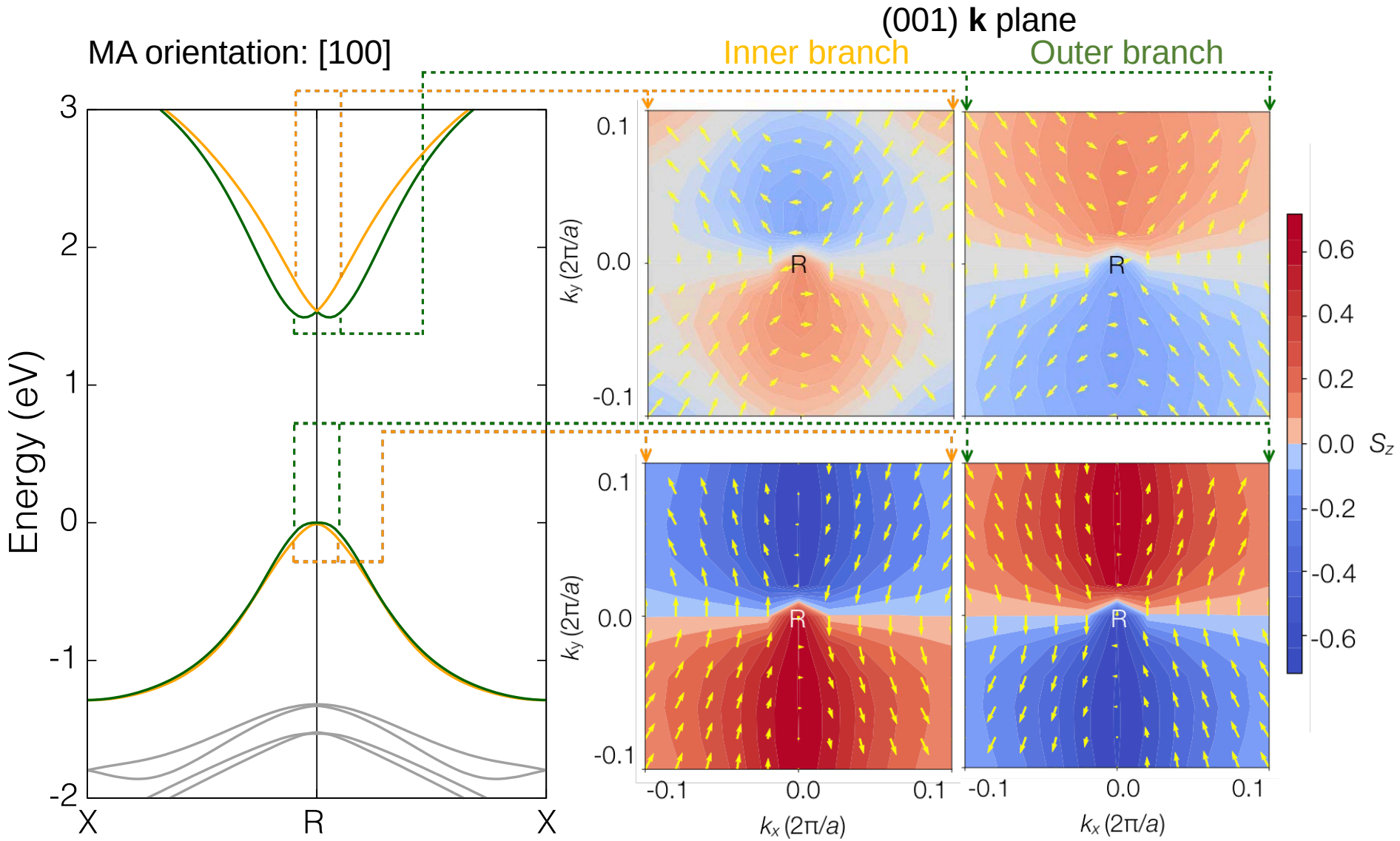

Phenomenological vs. First principles

spin orientation spin orientation

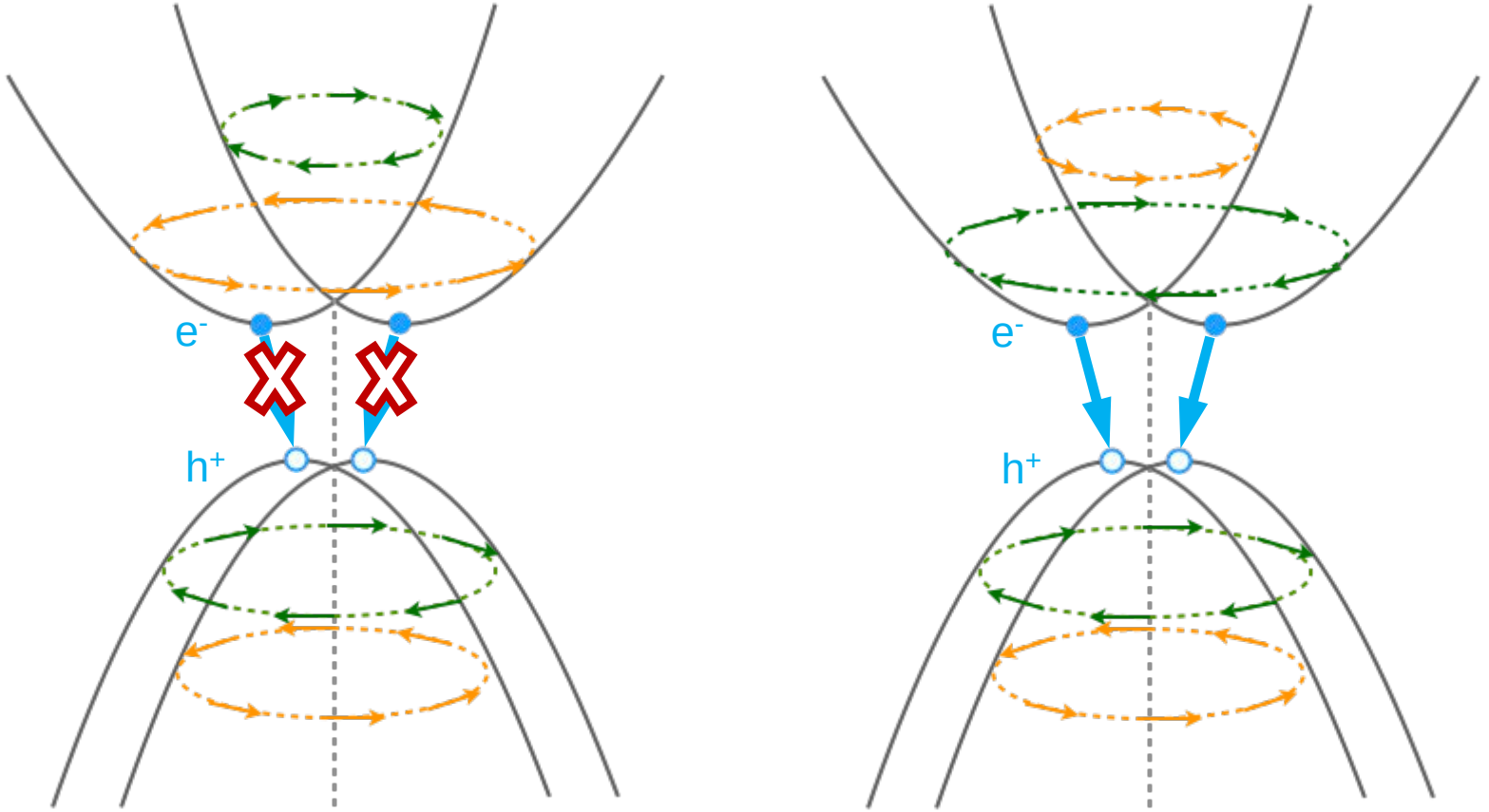

X. Zhang, J.-X. Shen, and C. G. Van de Walle, J. Phys. Chem. Lett. **9**, 2903 (2018).

Radiative recombination

- Fermi's Golden Rule:

Quasi-Fermi occupation

Matrix elements

$$B = \frac{n_r e^2}{\pi \epsilon_0 m_e^2 c^3 \hbar^2 n^2 V} \sum_{cv\mathbf{k}} f_{c\mathbf{k}} \left(1 - f_{v\mathbf{k}}\right) \left(\varepsilon_{c\mathbf{k}} - \varepsilon_{v\mathbf{k}}\right) \left|\mathbf{M}_{cv\mathbf{k}}\right|^2$$

Prefactor

Energy difference

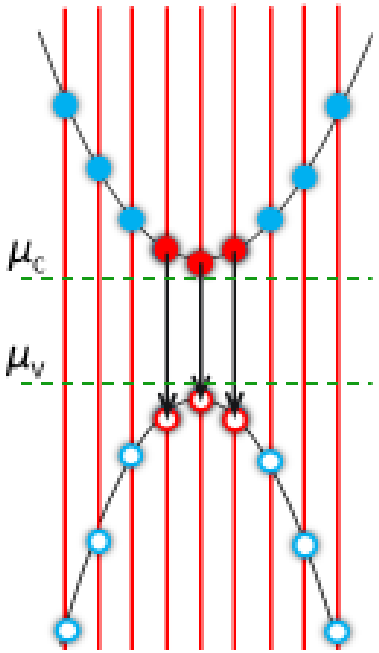

$$f_{c\mathbf{k}} = \frac{1}{1 + e^{\frac{E_{c\mathbf{k}} - \mu_c}{k_B T}}}$$

$$f_{v\mathbf{k}} = \frac{1}{1 + e^{\frac{E_{v\mathbf{k}} - \mu_v}{k_B T}}}$$

$$\left|\mathbf{M}_{cv\mathbf{k}}\right|^2 = \frac{1}{3} \sum_i \left|\langle \psi_c | p_i | \psi_v \rangle\right|^2$$

$$i = x, y, z$$

$$\sum_{c\mathbf{k}} f_{c\mathbf{k}} = \sum_{v\mathbf{k}} (1 - f_{v\mathbf{k}}) = n N_{\mathbf{k}} V_{\text{cell}}$$

Radiative recombination

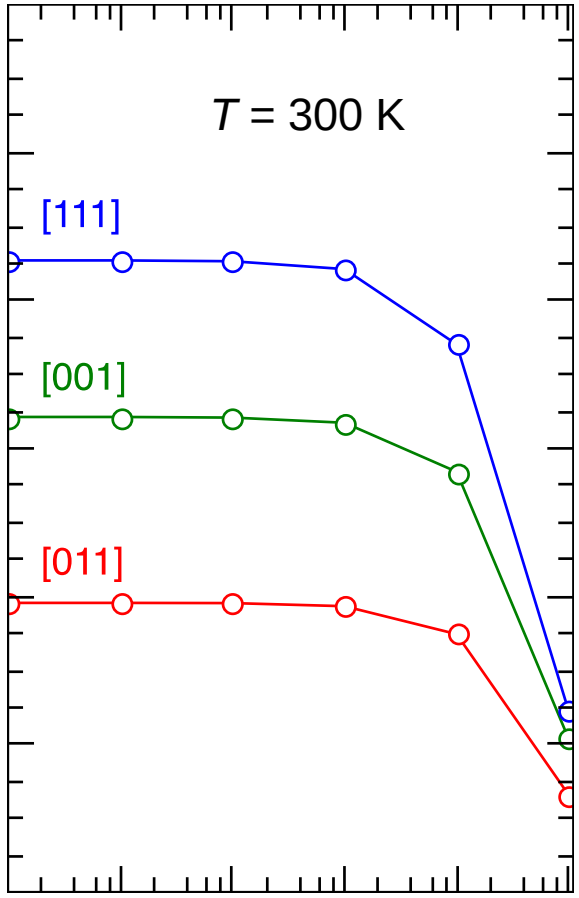

- Weak dependence on MA orientation (factor of 2)
- Limited impact of momentum mismatch on radiative recombination
- High radiative recombination coefficients ($\sim 10^{-10}$ cm^3s^{-1})
- Promising for light-emitting applications

H. Cho *et al.*, Science **350**, 1222 (2015).

Y.-H. Kim *et al.*, Adv. Mater. **27**, 1248 (2015).

X. Zhang, J.-X. Shen, W. Wang, and C. G. Van de Walle, ACS Energy Lett. **3**, 2329 (2018).

Recombination in halide perovskites

First-principles studies of recombination rates

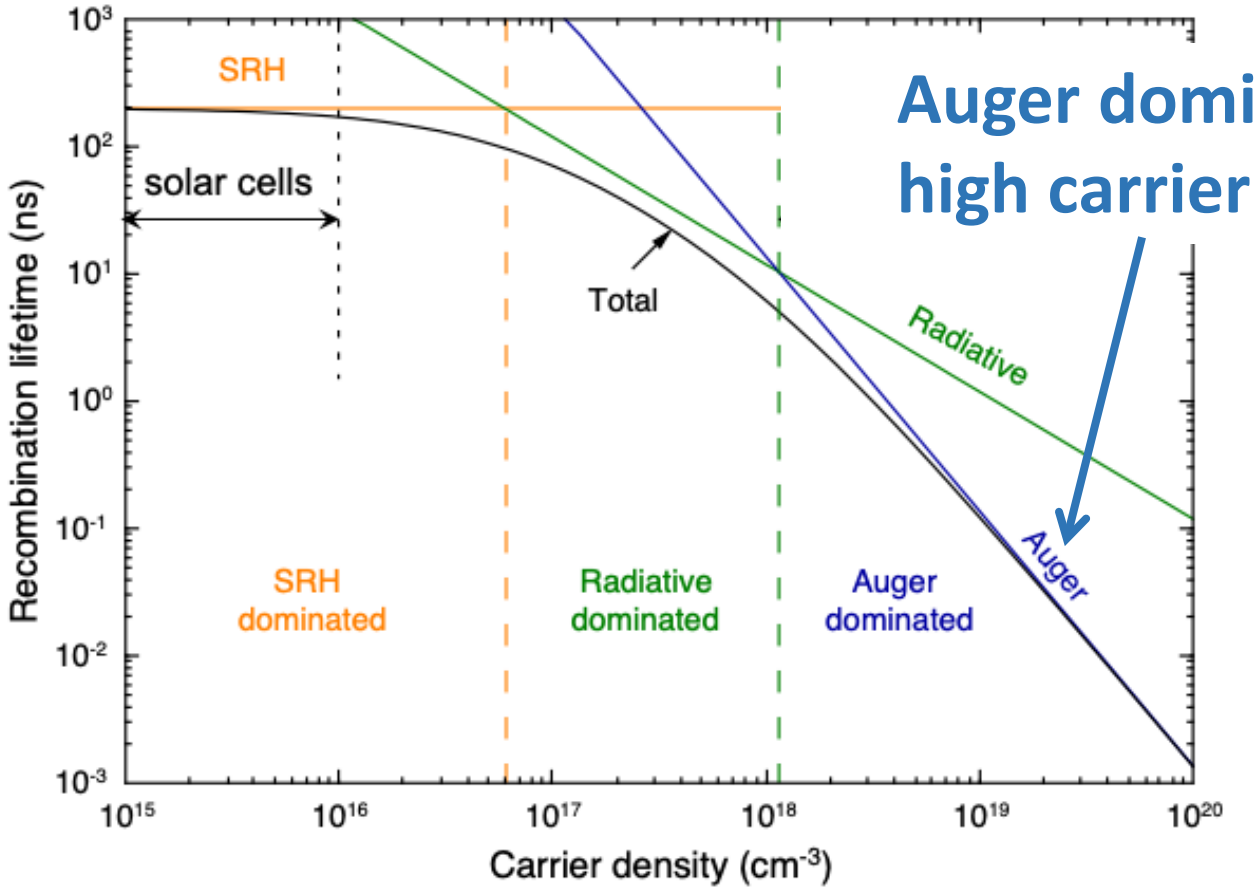

Auger dominates at high carrier densities

X. Zhang *et al.*, Adv. Energy Mater. **10**, 1902830 (2020).

X. Zhang *et al.*, J. Phys. Chem. Lett. **9**, 2903 (2018).

X. Zhang *et al.*, ACS Energy Lett. **3**, 2329 (2018).

J.-X. Shen *et al.*, Adv. Energy Mater. **8**, 1801027 (2018).

Auger recombination

- Fermi's Golden Rule:

Matrix elements

$$C = \frac{2\pi}{\hbar n^3} \sum_{1234} f_1 f_2 (1 - f_3)(1 - f_4) |M_{1234}|^2 \delta(\varepsilon_1 + \varepsilon_2 - \varepsilon_3 - \varepsilon_4)$$

Quasi-Fermi occupation

Energy conservation

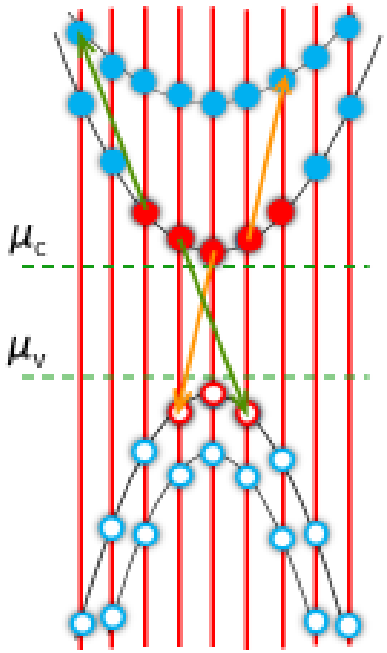

- First-principles calculations for very dense **k**-point grid, e.g., 50 x 50 x 50 for sampling the first Brillouin zone
- Directly search for all possible Auger events that conserve energy and momentum
- Usually on the order of a few tens of millions of possible events

$$|M_{1234}|^2 = \left|M^d_{1234} - M^x_{124}\right|^2 + \left|M^d_{124}\right|^2 + |M^x_{1234}|^2$$

Direct process: $M^d_{1234} = \langle \psi_1 \psi_2 | W | \psi_3 \psi_4 \rangle$

Exchange process: $M^x_{1234} = \langle \psi_1 \psi_2 | W | \psi_4 \psi_3 \rangle$

Auger recombination

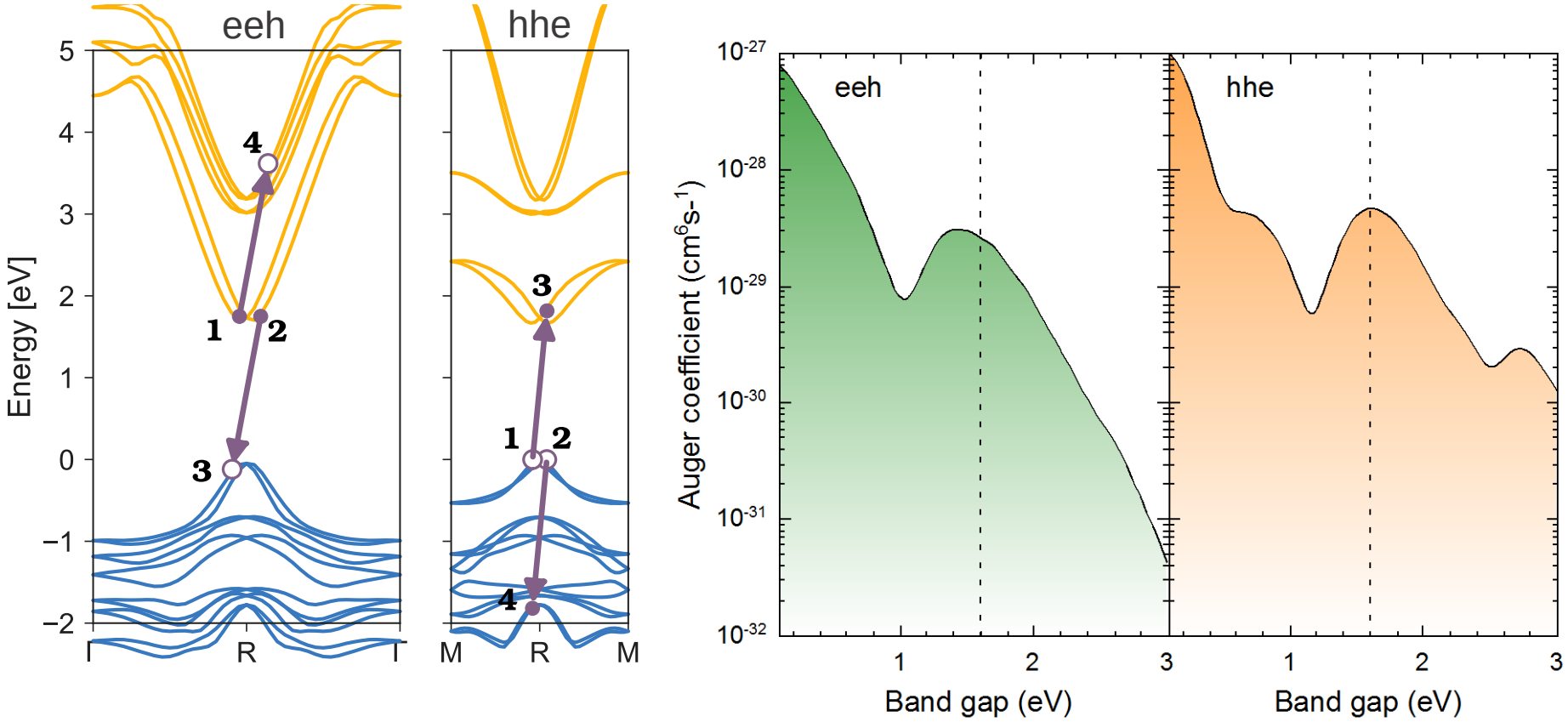

- Theory: C_{tot} = 7 x 10^{-29} cm^6s^{-1} at E_g = 1.6 eV
- Exp.:10^{-29} ~ 10^{-28} cm^6s^{-1} [R. L. Milot *et al.*, Adv. Funct. Mater. **25**, 6218 (2015).]

Auger recombination

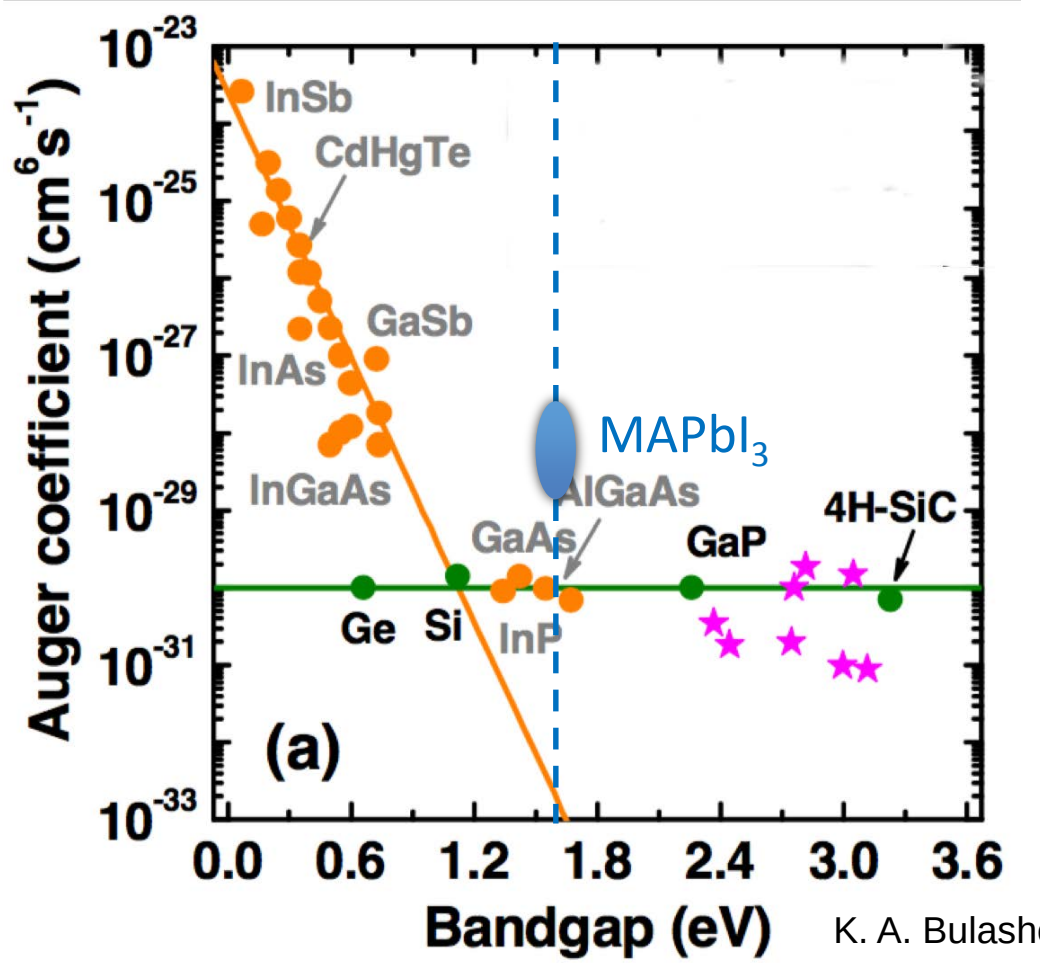

K. A. Bulashevich *et al*., Phys. Stat. Sol. (c) **5**, 2066 (2008).

- $MAPbI_3$ has a much greater Auger coefficient ~100x

Origin of strong Auger

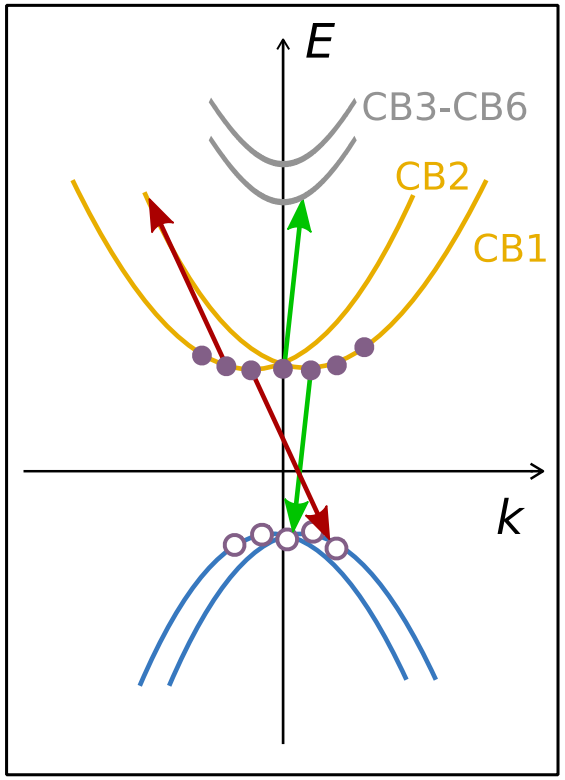

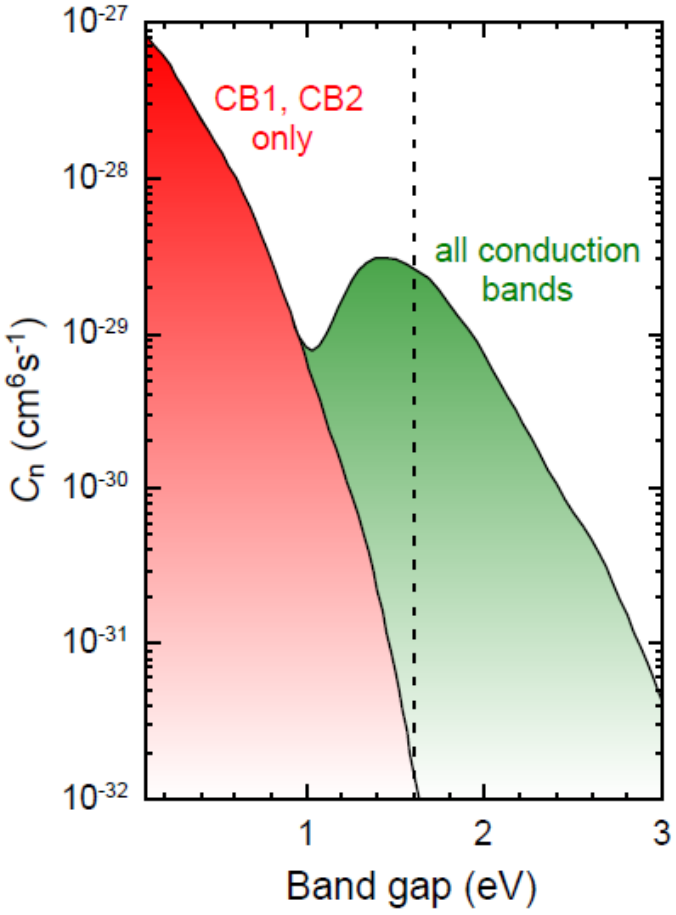

J.-X. Shen, X. Zhang, S. Das, E. Kioupakis, and C. G. Van de Walle, Adv. Energy Mater. **8**, 1801027 (2018).

Spin-orbit energy splitting

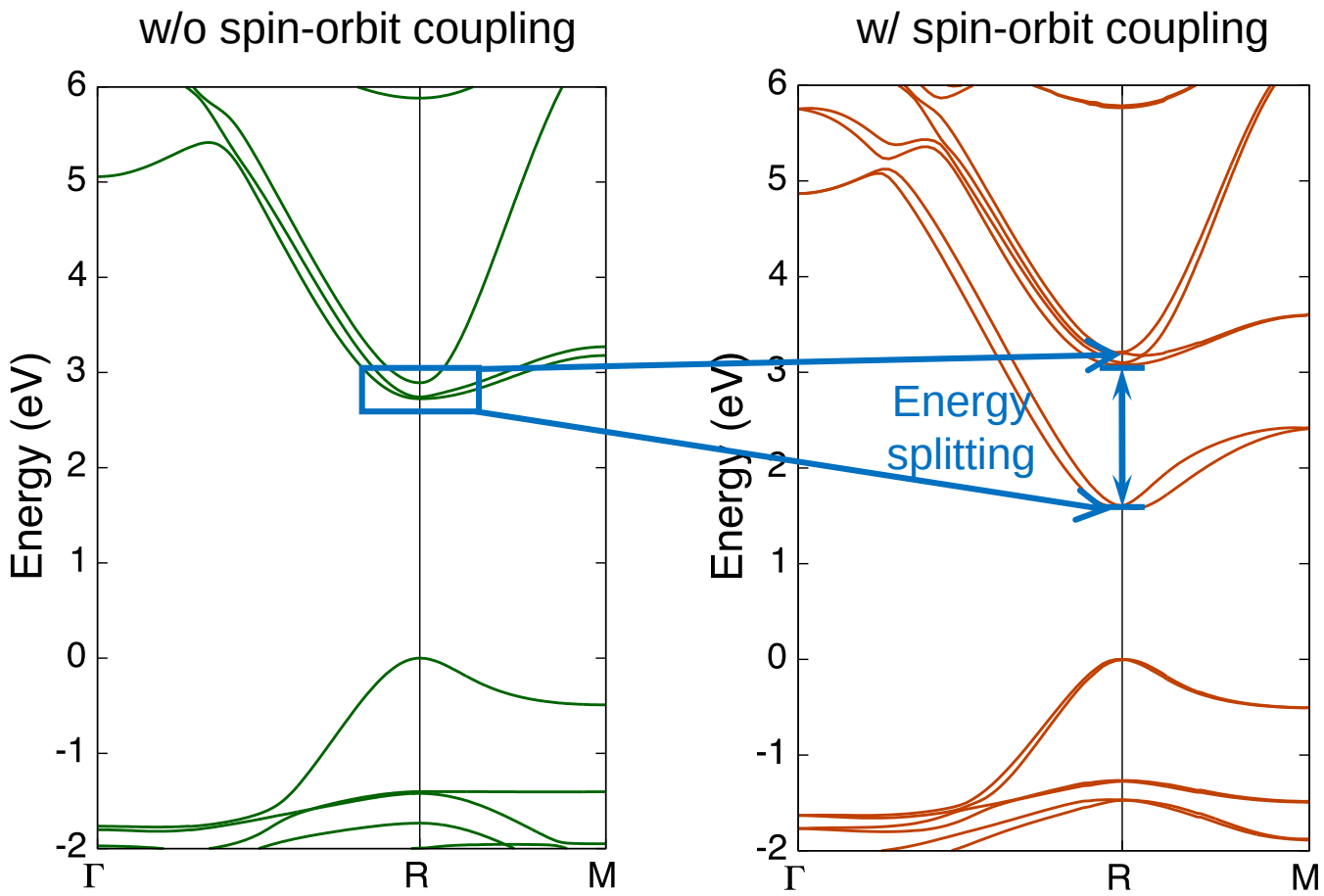

Energy splitting in conduction bands causes resonance for eeh Auger

Band-structure engineering

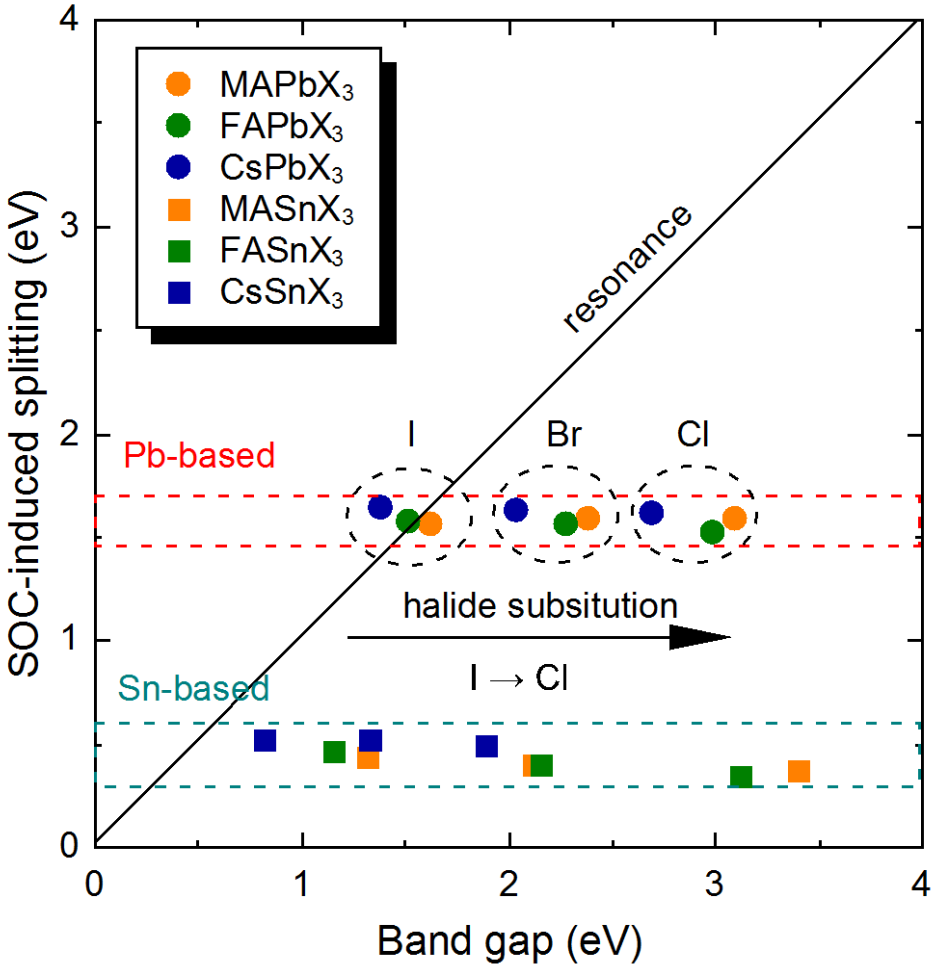

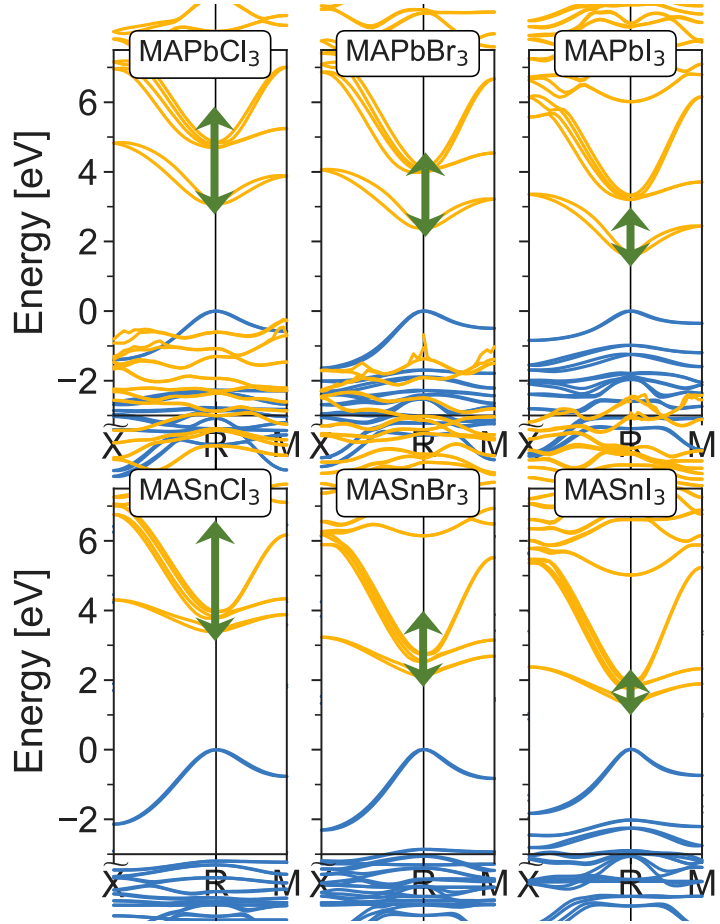

X. Zhang, J.-X. Shen, and C. G. Van de Walle, Adv. Energy Mater. **9**, 1902830 (2019).

- X-site substitution can suppress eeh Auger

What about hhe Auger?

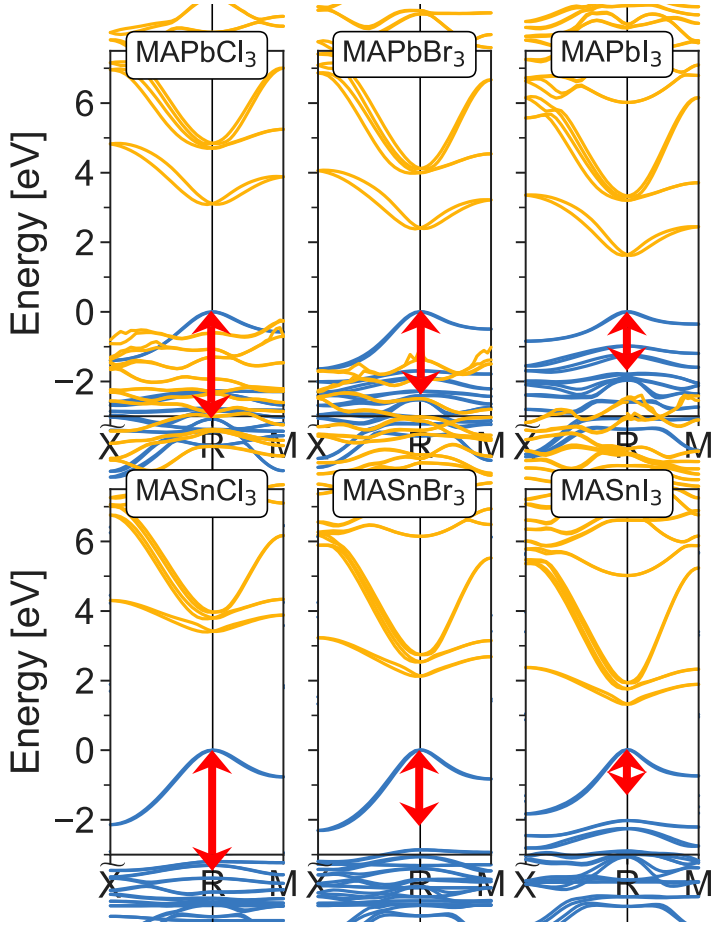

X. Zhang, J.-X. Shen, and C. G. Van de Walle, Adv. Energy Mater. **9**, 1902830 (2019).

- B-site substitution allows suppressing hhe Auger

Suppressing lattice distortions

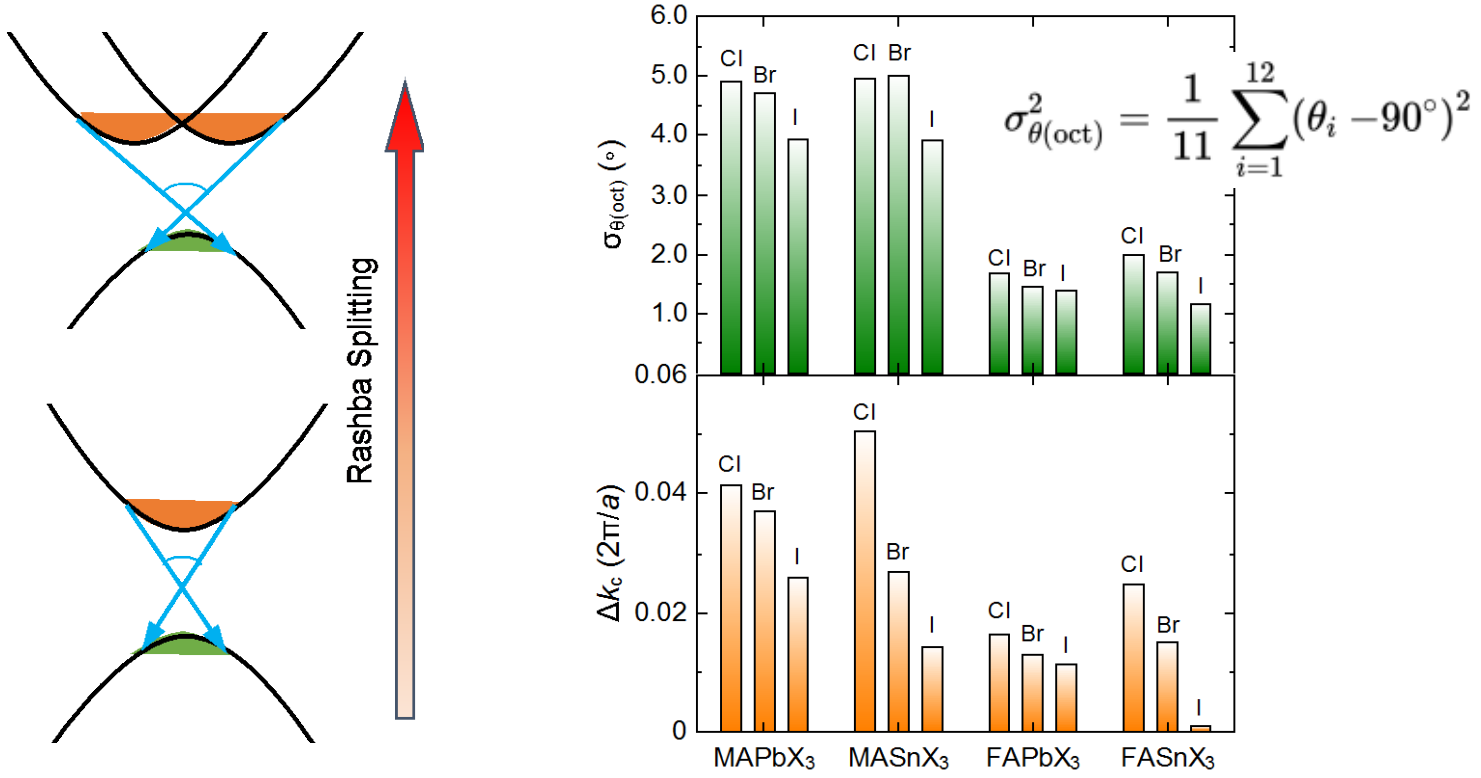

X. Zhang, J.-X. Shen, and C. G. Van de Walle, Adv. Energy Mater. **9**, 1902830 (2019).

- Tunable lattice distortion and Rashba splitting by chemical substitution

Suppressing lattice distortions

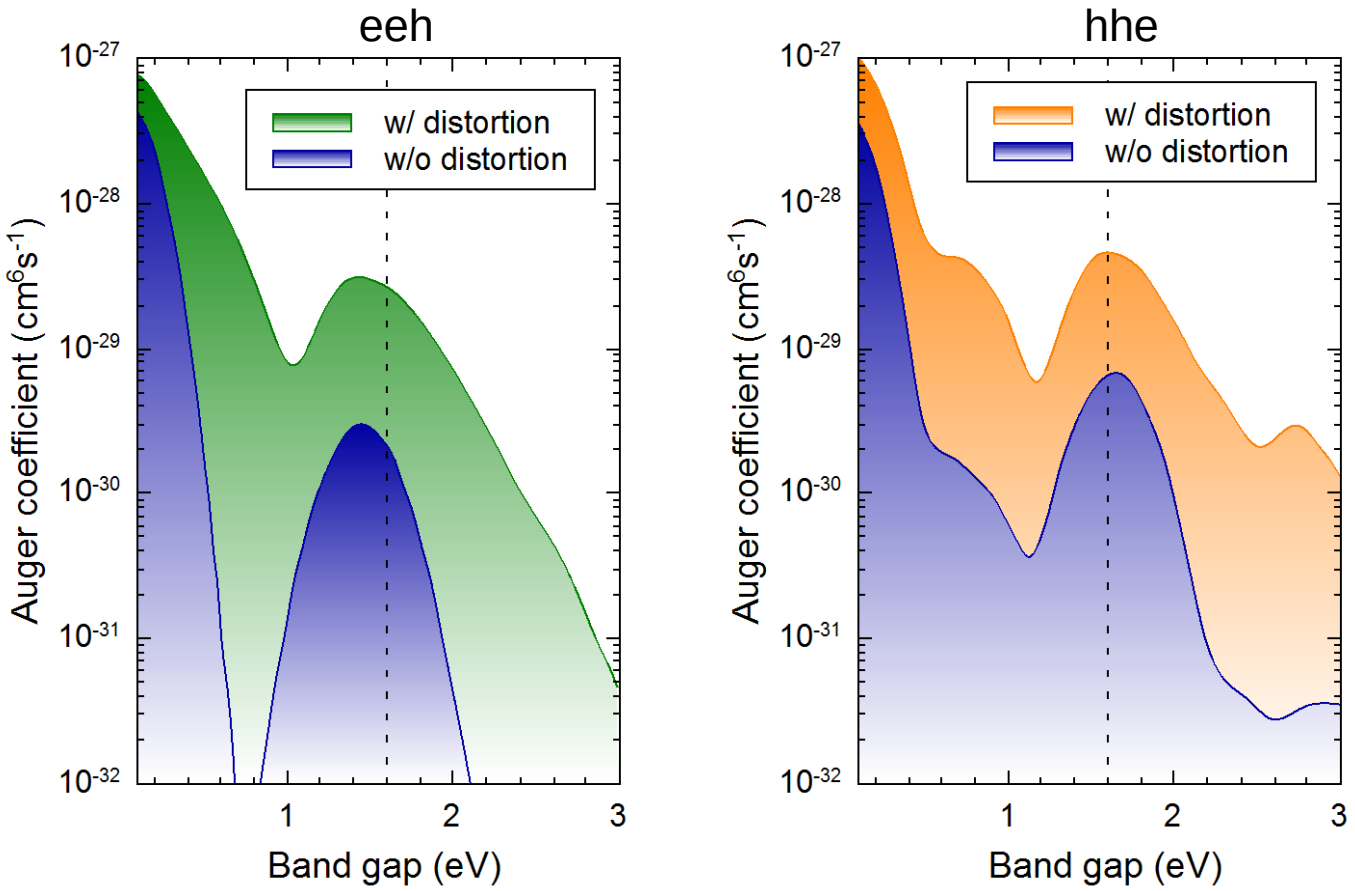

- Suppressing lattice distortions and thus the Rashba splitting reduces Auger by one order of magnitude

Recombination in halide perovskites

First-principles studies of recombination rates

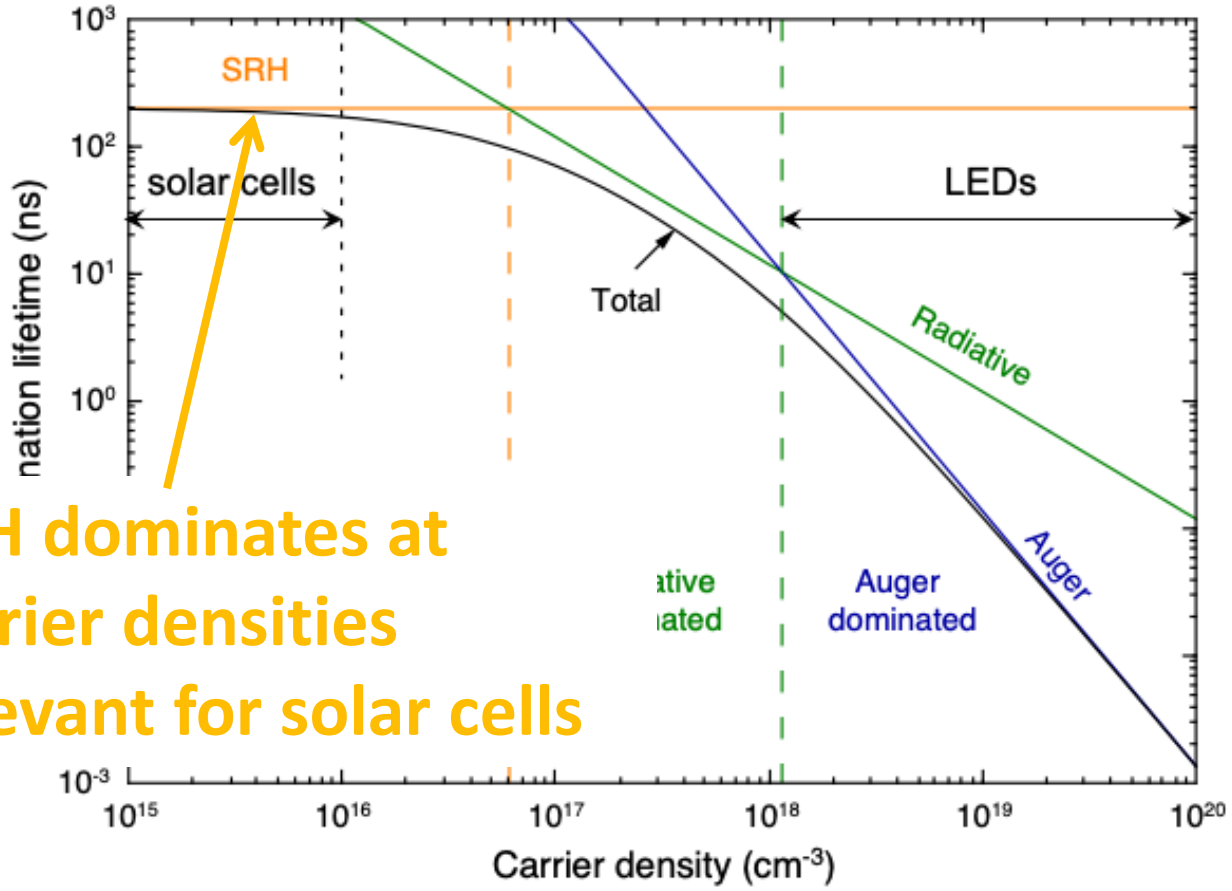

SRH dominates at carrier densities relevant for solar cells

X. Zhang *et al.*, Adv. Energy Mater. **10**, 1902830 (2020).

- Defect-assisted ("SRH") recombination limits efficiency

X. Zhang *et al.*, J. Phys. Chem. Lett. **9**, 2903 (2018).

X. Zhang *et al.*, ACS Energy Lett. **3**, 2329 (2018).

J.-X. Shen *et al.*, Adv. Energy Mater. **8**, 1801027 (2018).

“Defect tolerance”

- “Defect tolerance”: defects are present, but do not cause strong nonradiative carrier recombination
- Concept emerged from early, less accurate, first-principles calculations for defects in $MAPbI_3$
  - none of the relevant defects had levels deep in the band gap
- Commonly invoked to explain the high efficiency of perovskite solar cells
- However, deep-level defects with concentrations ~10^{15} cm^{-3} are observed experimentally!

- Thermally stimulated current (TSC)

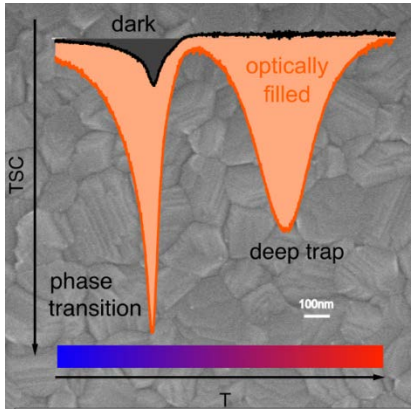

A. Baumann *et al*., J. Phys. Chem. Lett. **6**, 2350 (2015).

- Deep level transient spectroscopy (DLTS)

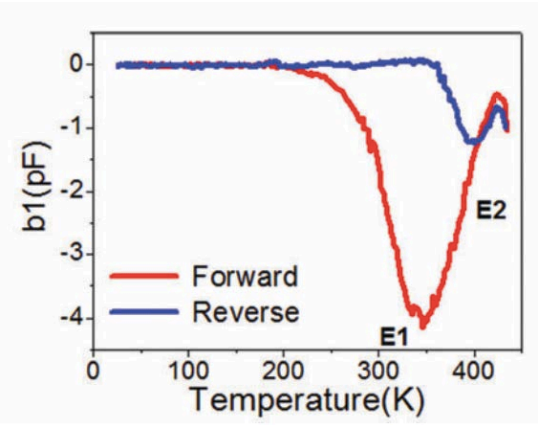

S. Heo *et al*., Energy Environ. Sci. **10**, 1128 (2017).

Point defects in halide perovskites

First-principles calculations of formation energies and defect levels

C. Freysoldt *et al*., Rev. Mod. Phys. **86**, 253 (2014).

Example: iodine interstitial (I_i)

(chemical potential of I)

Fermi level
(chemical potential of electrons)

$$E^f[\mathrm{I}_i^q] = E_{\mathrm{tot}}[\mathrm{I}_i^q] - E_{\mathrm{tot}}[\mathrm{bulk}] - \mu_{\mathrm{I}} + qE_{\mathrm{F}}$$

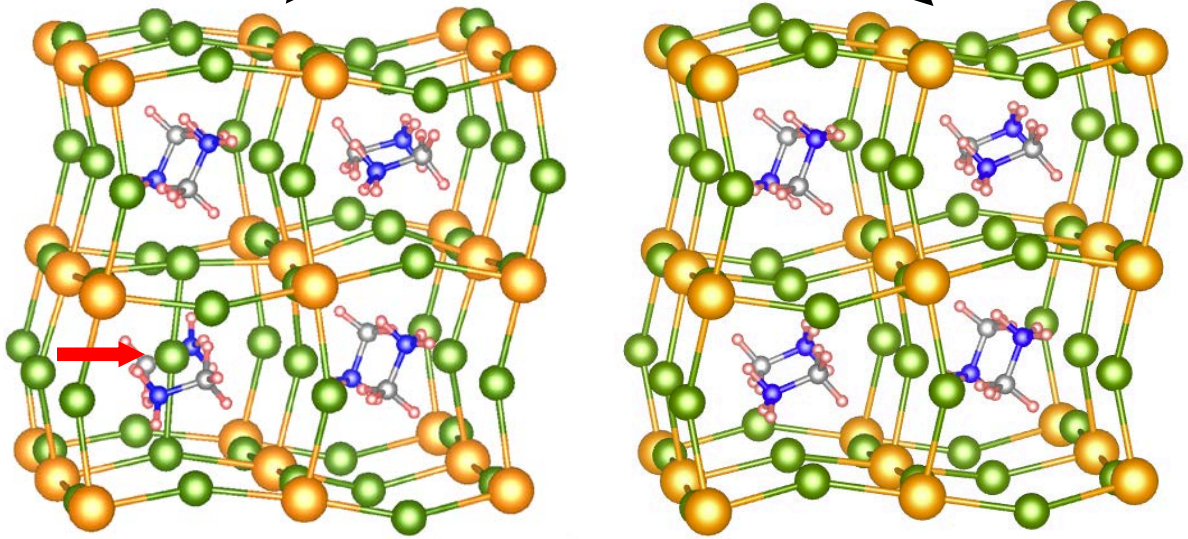

q=+1

- Density functional theory
- Hybrid functional
  - J. Heyd, G. E. Scuseria, and M. Ernzerhof, J. Chem. Phys. **118**, 8207 (2003).
- Spin-orbit coupling
- Supercells, atomic relaxation

Defect concentration: $N_{\mathrm{def}} = N_{\mathrm{sites}} e^{-E^f/k_{\mathrm{B}}T}$

Defect-assisted recombination in halide perovskites

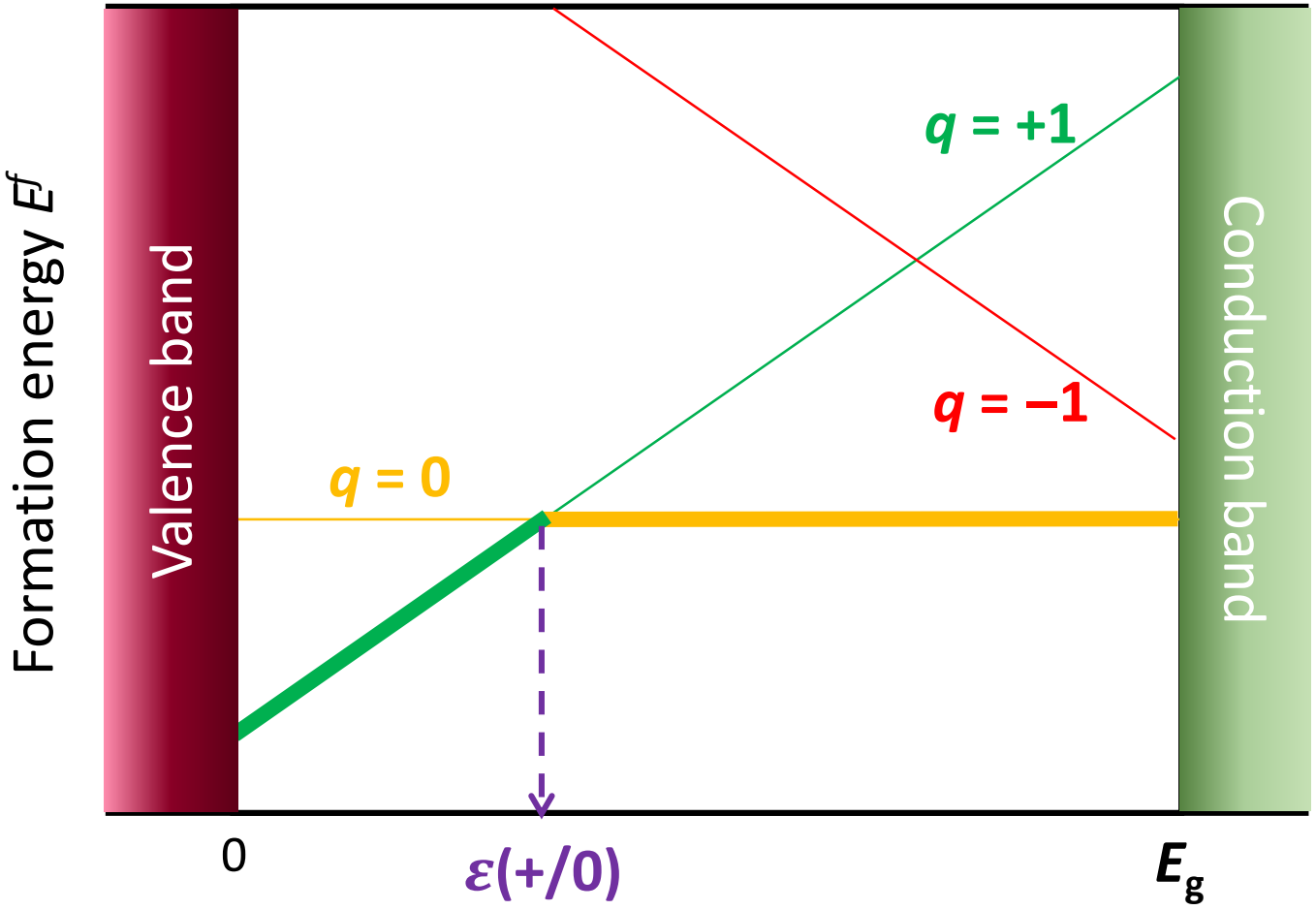

ε(+/0): charge-state transition level relevant for SRH recombination

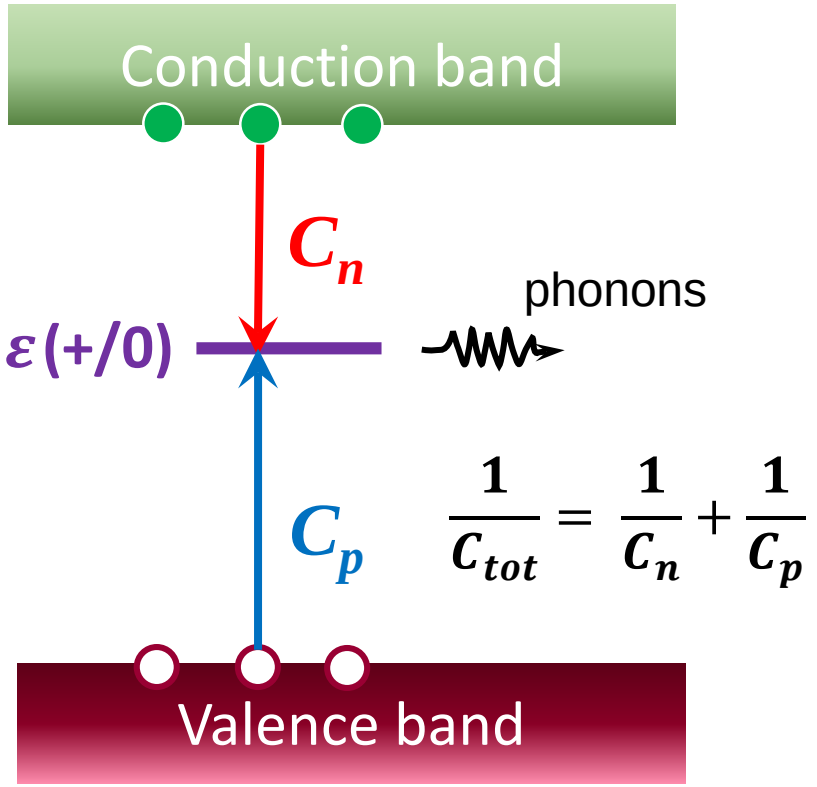

- Usually, $C \propto e^{-\Delta E}$
- Mid-gap defects have best balance between C_n and C_p

Configuration coordinate diagram

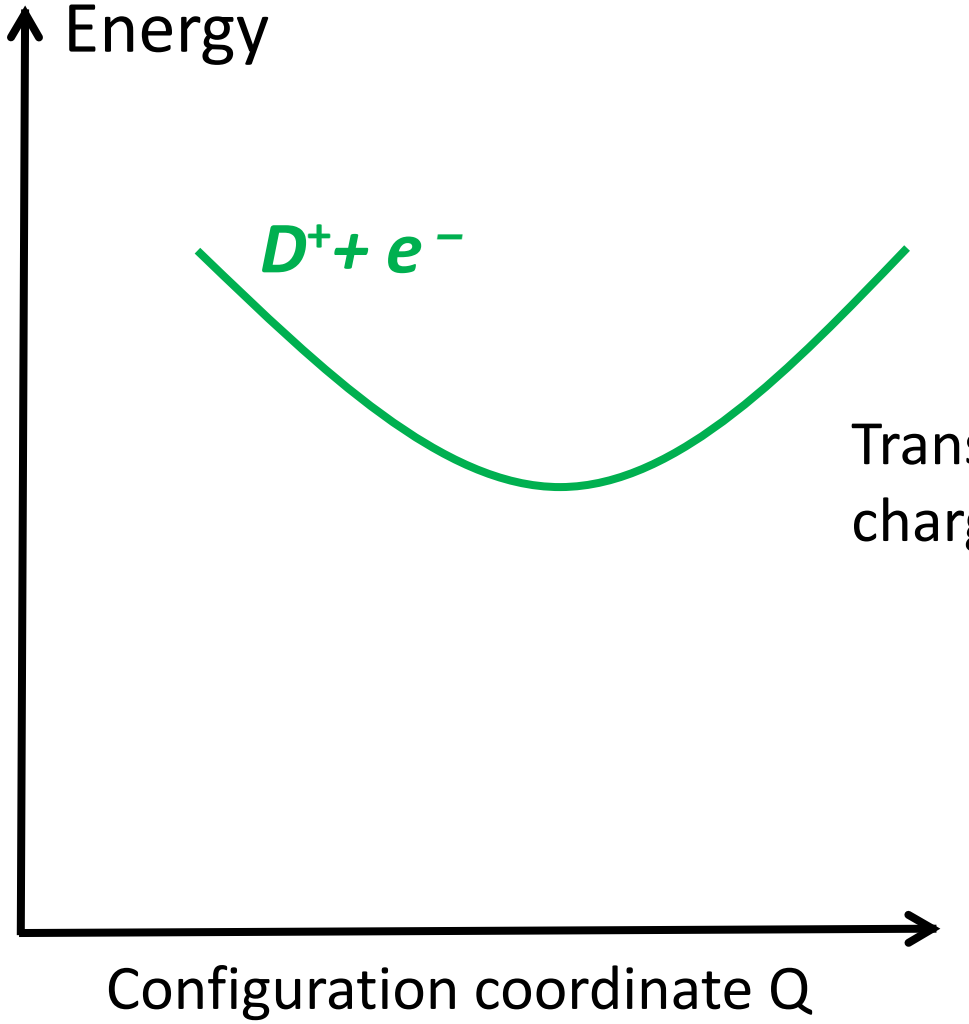

Transition between charge states D^+ and D^0

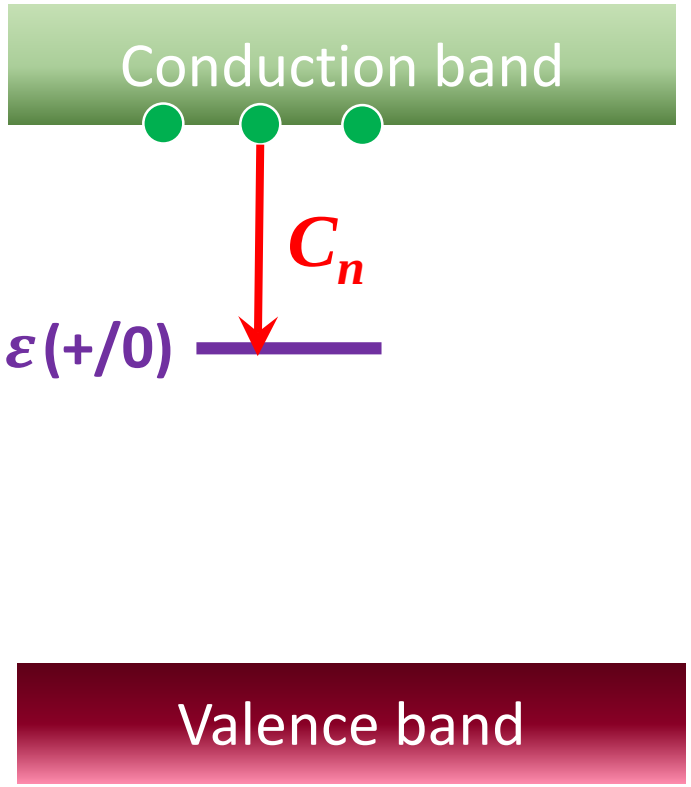

Configuration coordinate diagram

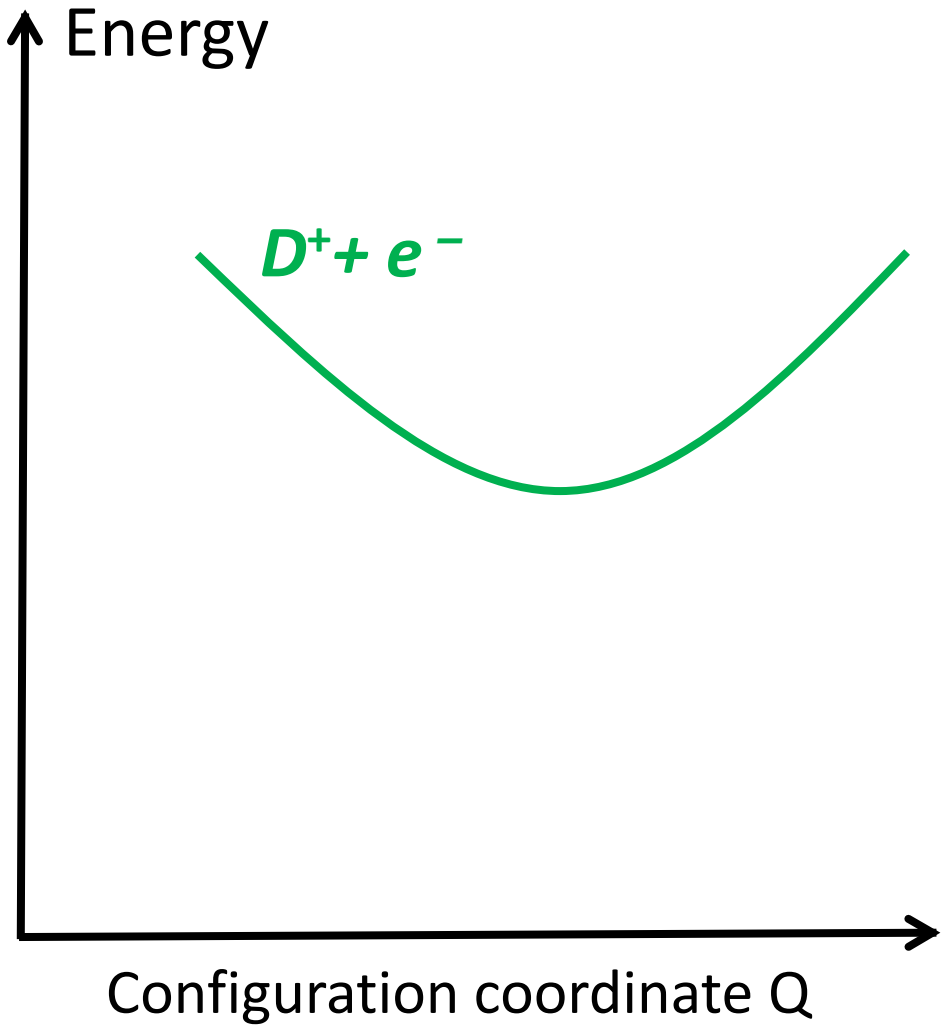

Energy depends on
atomic configuration

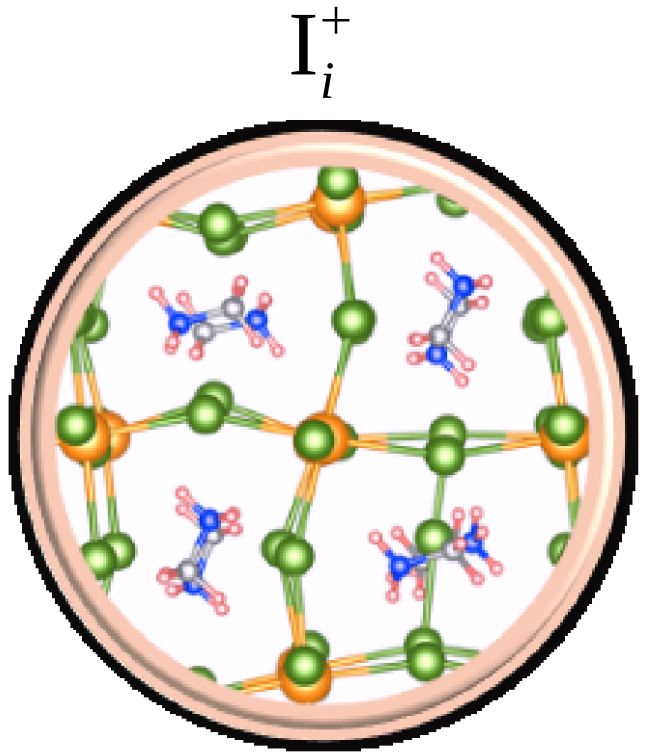

Configuration coordinate diagram

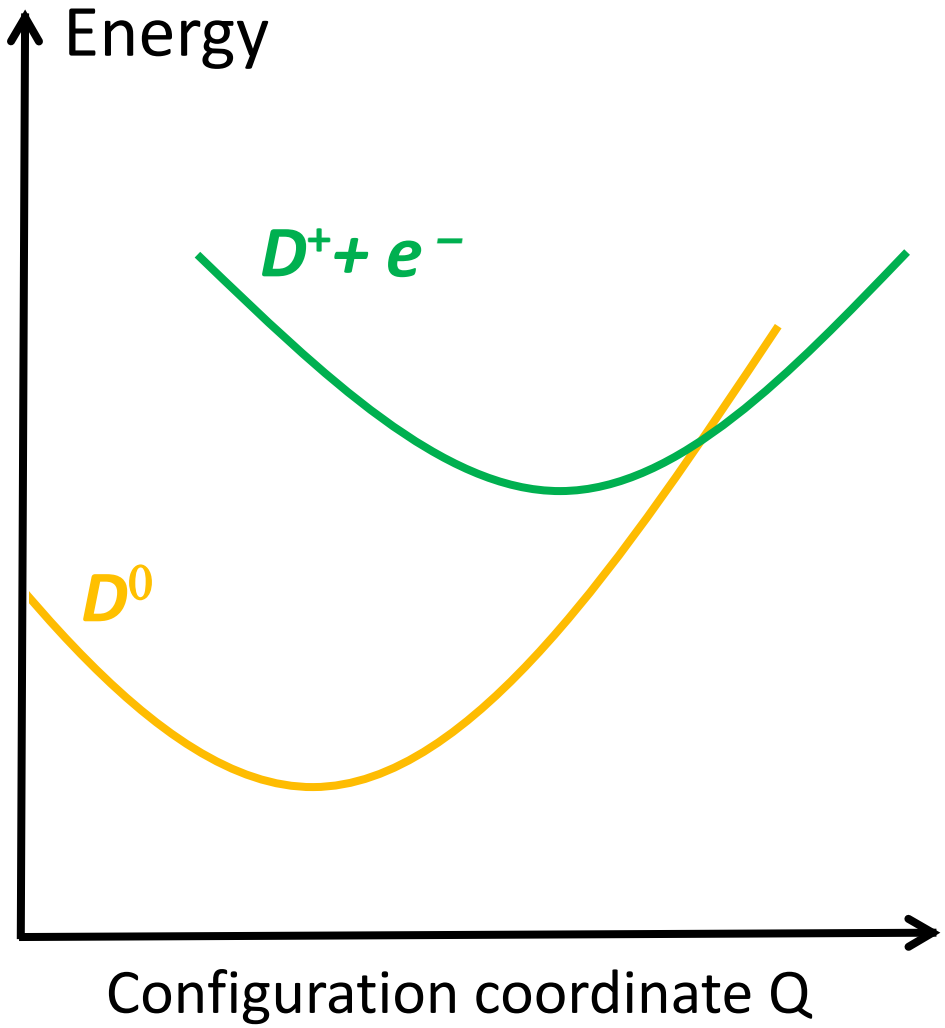

Energy depends on atomic configuration

Charge state D^0 has different atomic configuration from D^+

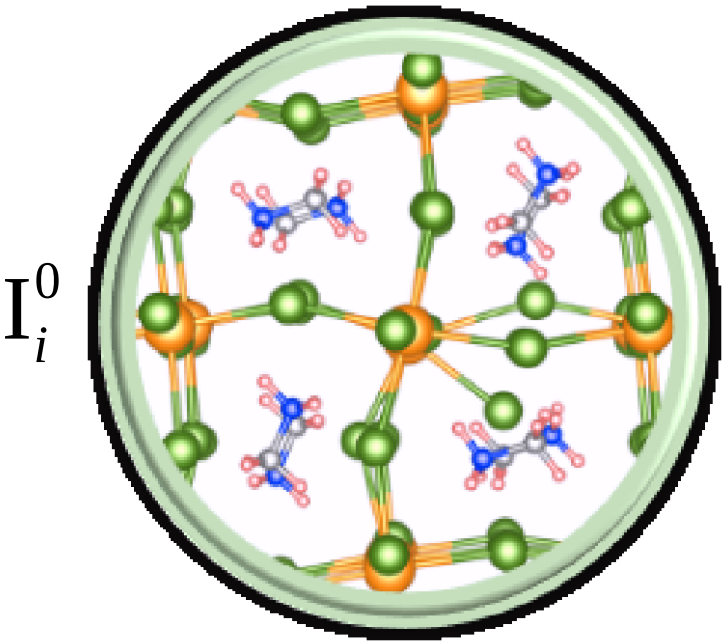

Configuration coordinate diagram

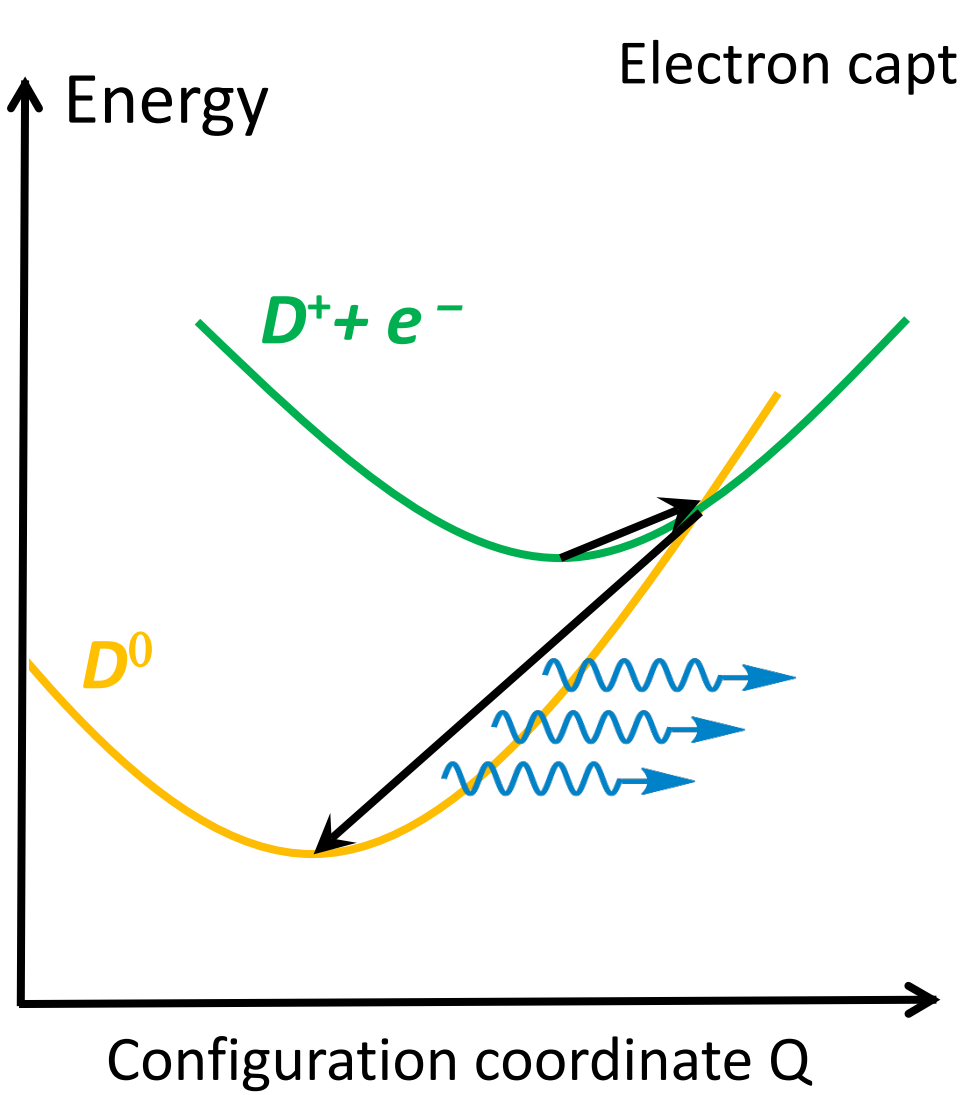

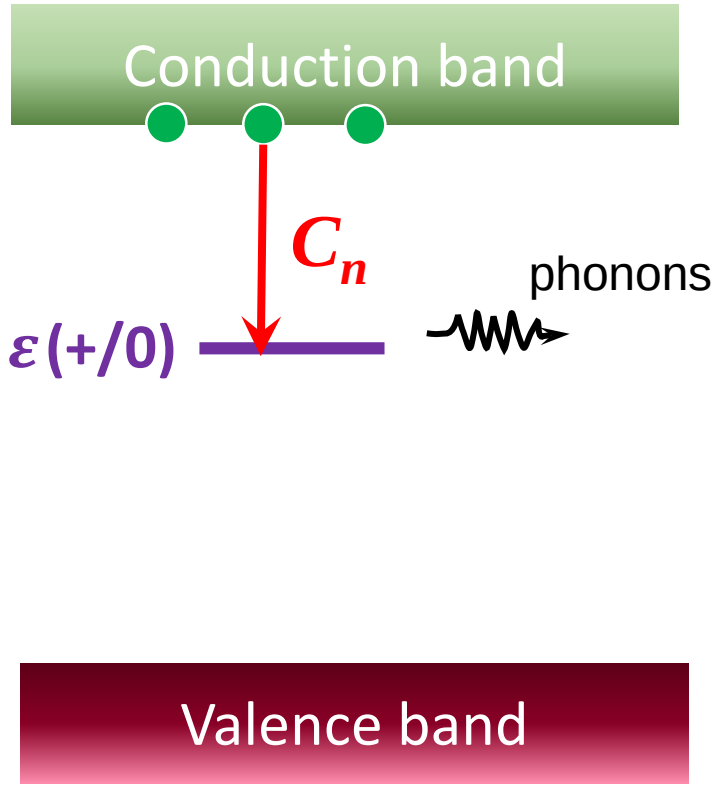

Configuration coordinate diagram

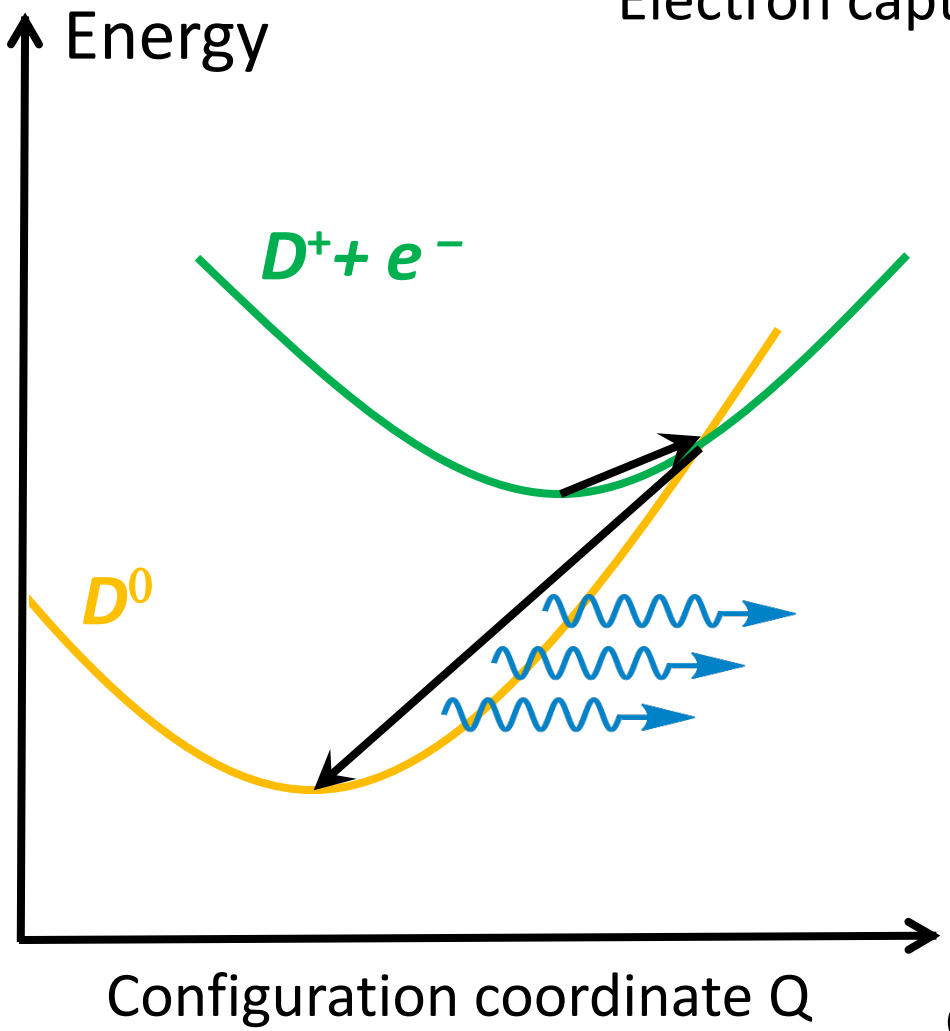

Configuration coordinate diagram from first principles

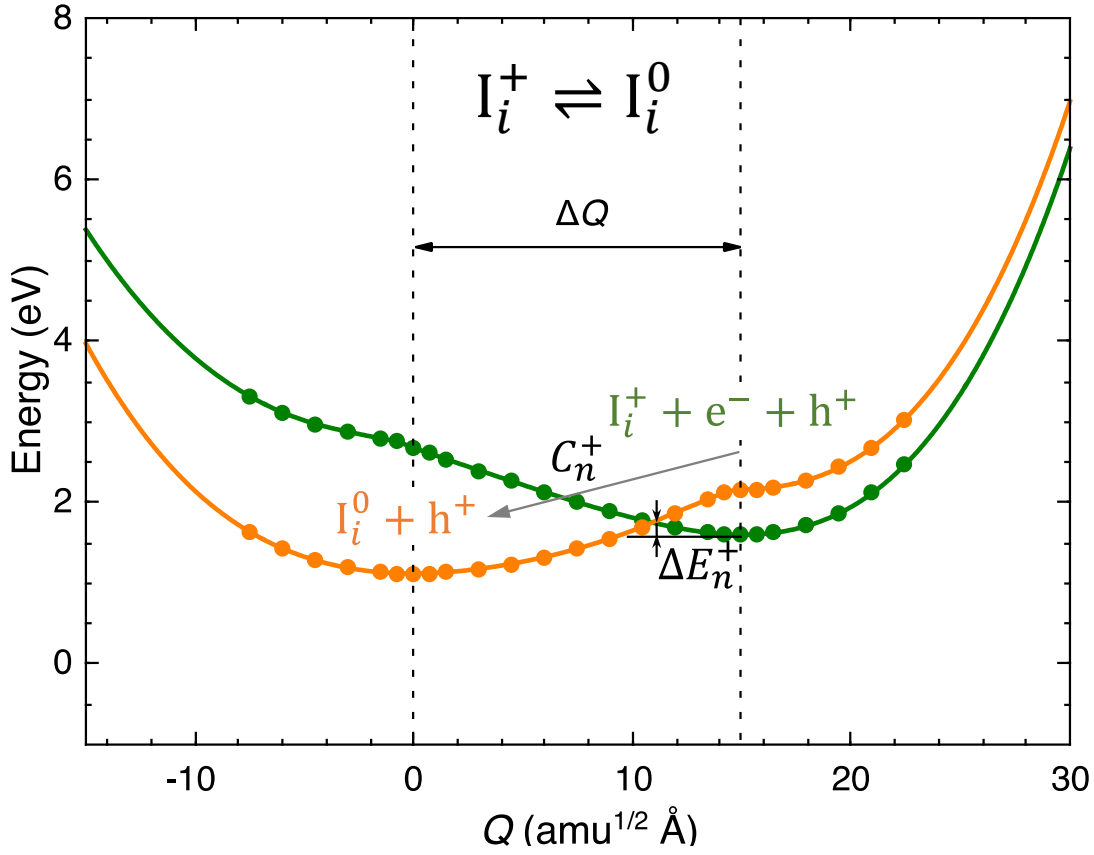

Generalized coordinate: $Q = \sqrt{\sum_{\alpha} m_{\alpha} \left(\mathbf{R}_{\alpha} - \mathbf{R}_{\mathrm{f};\alpha}\right)^2}$

Prominent defect: iodine interstitial

- Low formation energy → high concentration
- Four capture processes

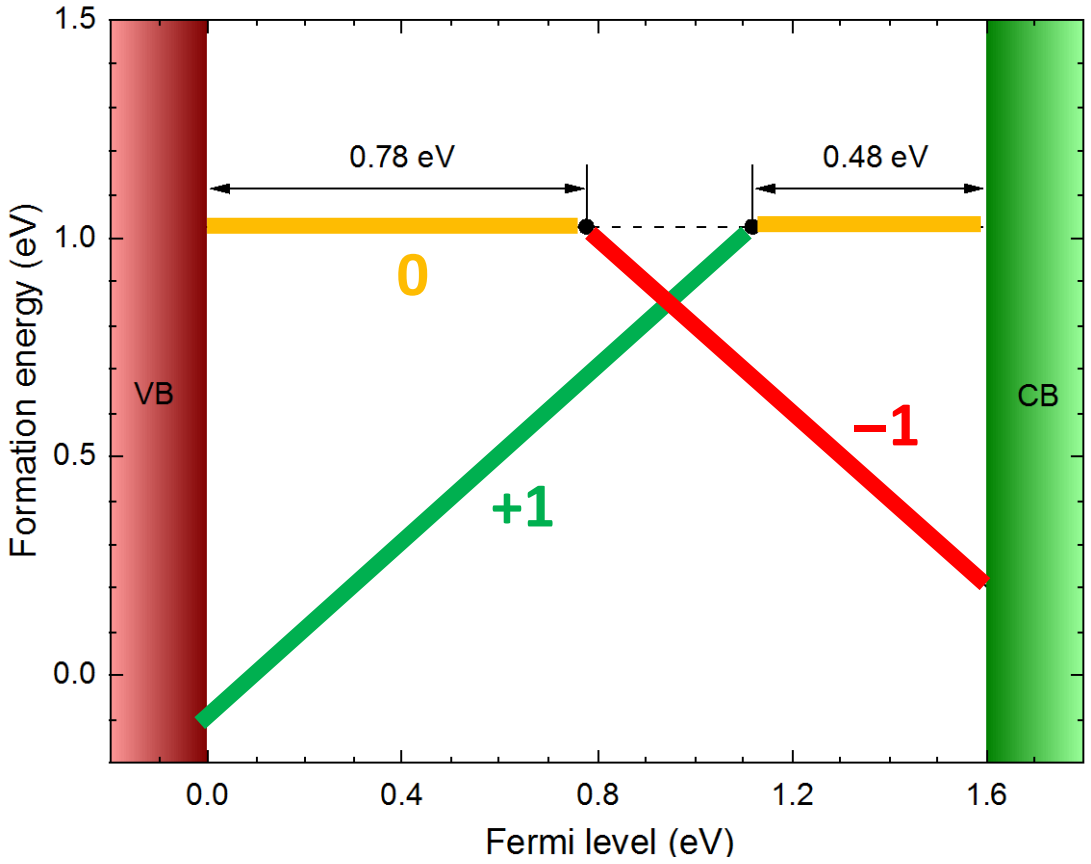

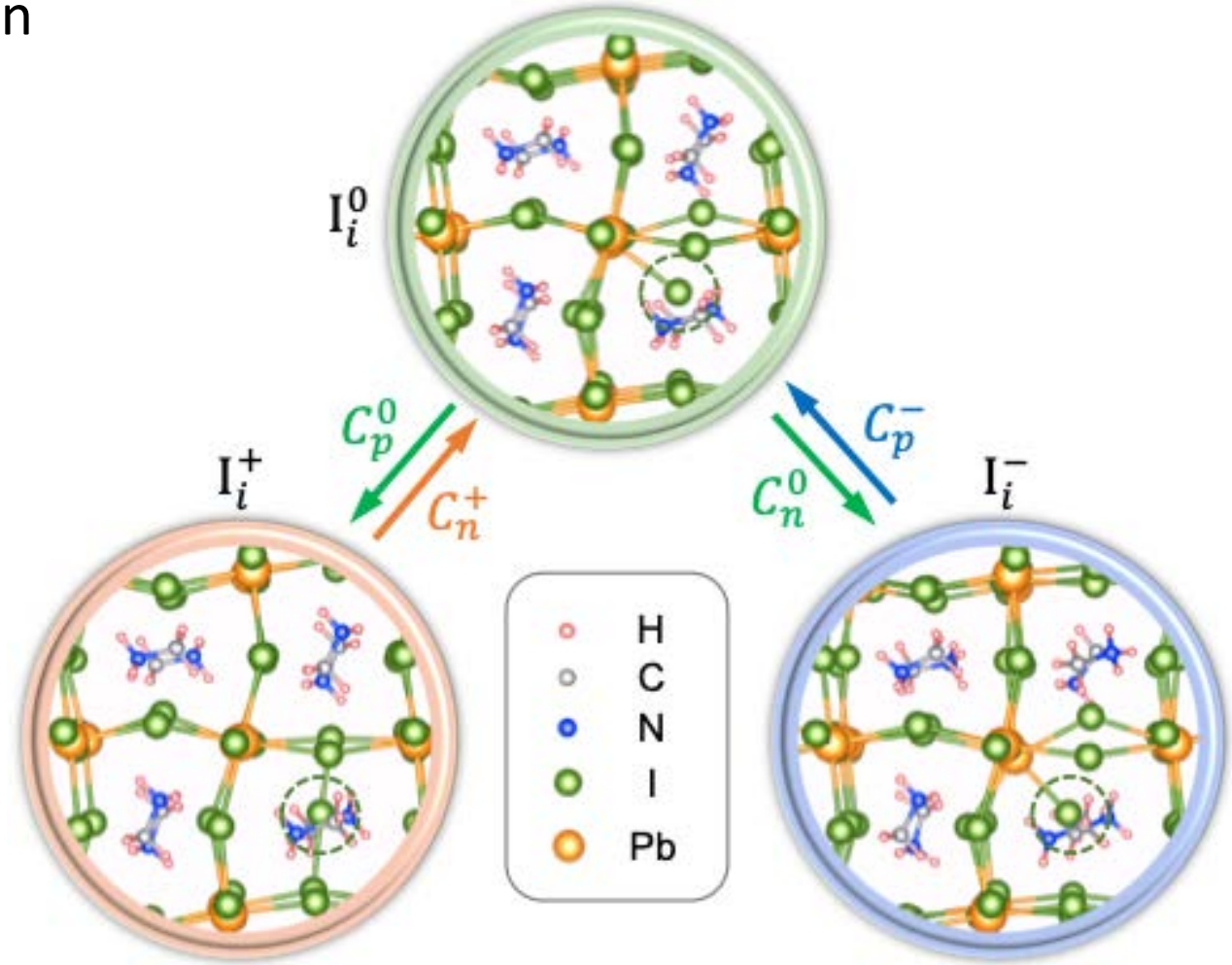

X. Zhang *et al.*, Phys. Rev. B **101**, 140101 (2020).

Configuration coordinate diagram: $I_i^+ \rightleftharpoons I_i^0$

- Generally small capture barriers
  → high capture coefficients
- Capture coefficients do not decrease as expected with energy difference from band edge (i.e., $C \propto e^{-\Delta E}$)
- Two reasons:
  - Anharmonicity
  - "Marcus inverted region"

X. Zhang *et al.*, Phys. Rev. B **101**, 140101 (2020).

Configuration coordinate diagram from first principles

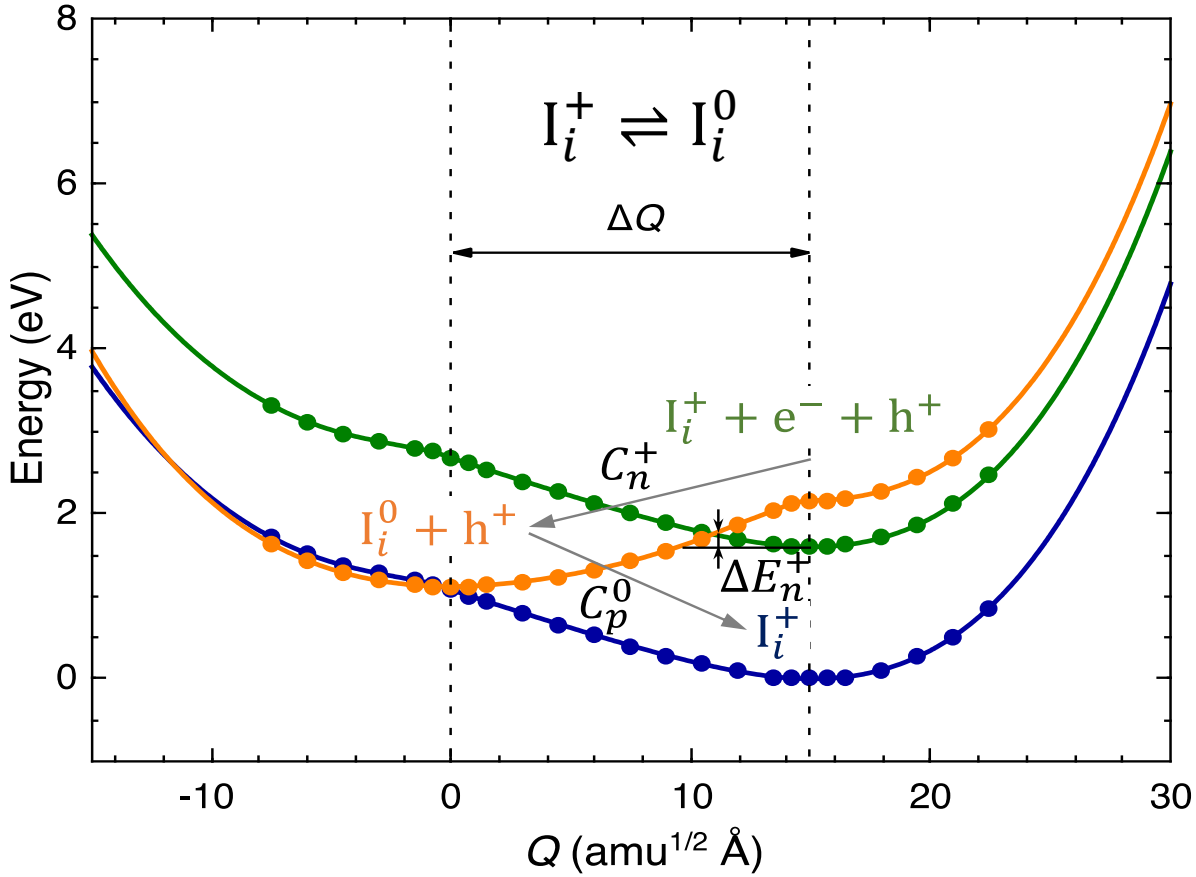

Capture coefficients

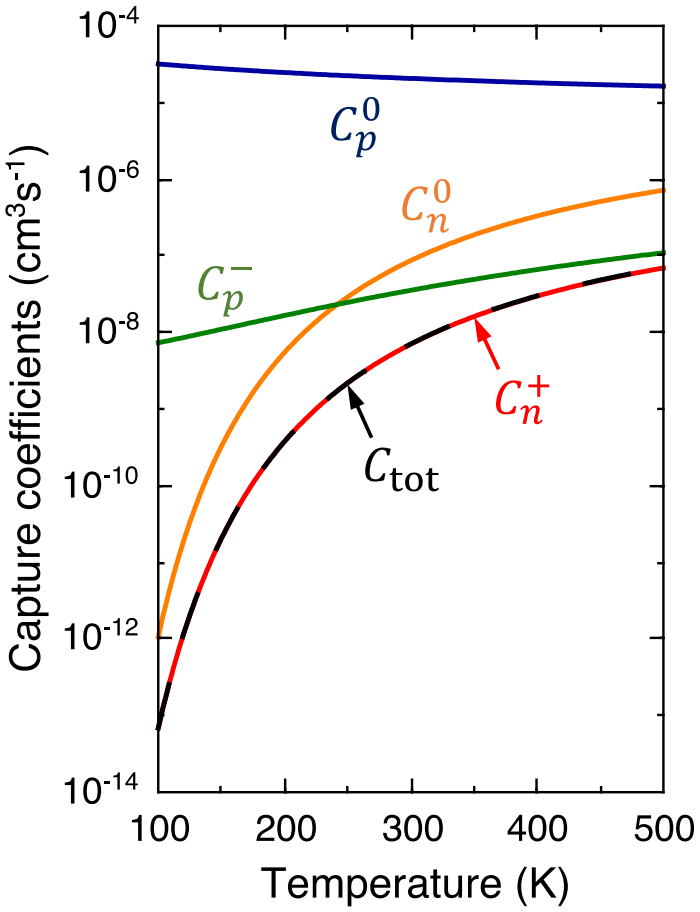

- $\mathrm{I}_i^+ \rightleftharpoons \mathrm{I}_i^0$ and $\mathrm{I}_i^0 \rightleftharpoons \mathrm{I}_i^-$ charge-state transitions
- Four capture processes
- Total capture coefficient:

$$C_{\rm tot} = \frac{C_n^0 + C_p^0}{1 + \frac{C_n^0}{C_p^-} + \frac{C_p^0}{C_n^+}}$$

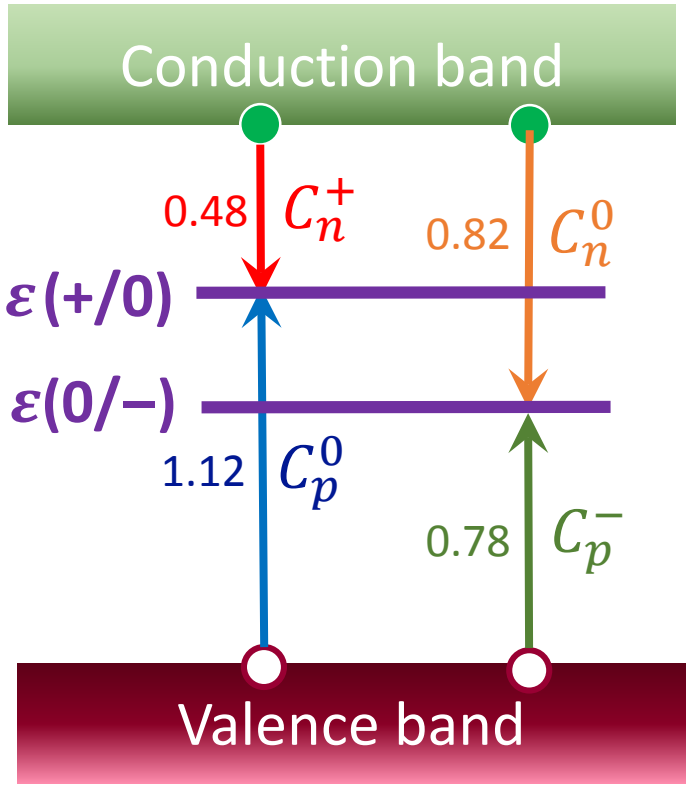

X. Zhang *et al.*, Phys. Rev. B **101**, 140101 (2020).

Capture coefficients

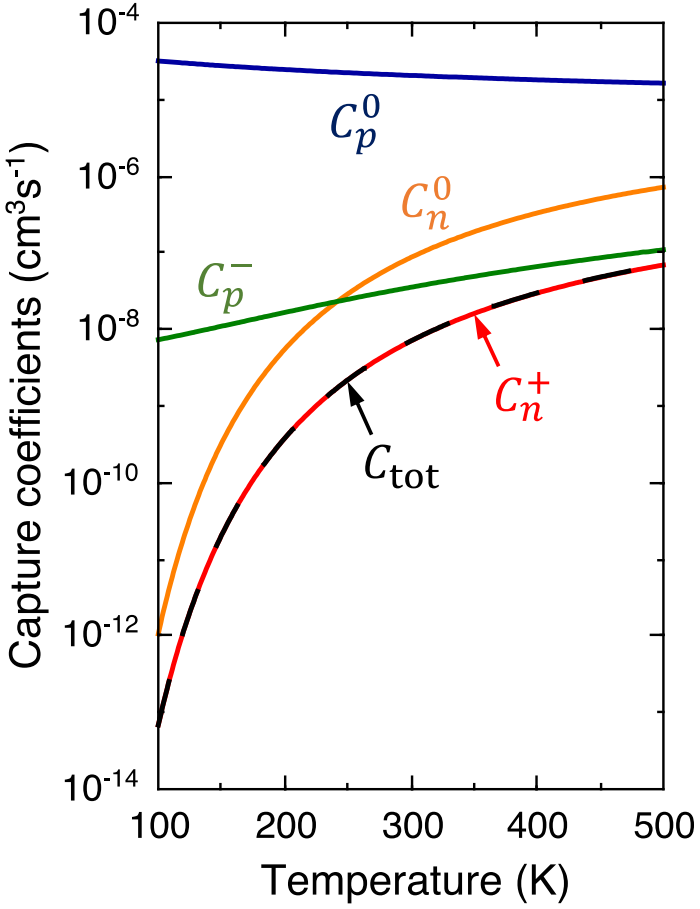

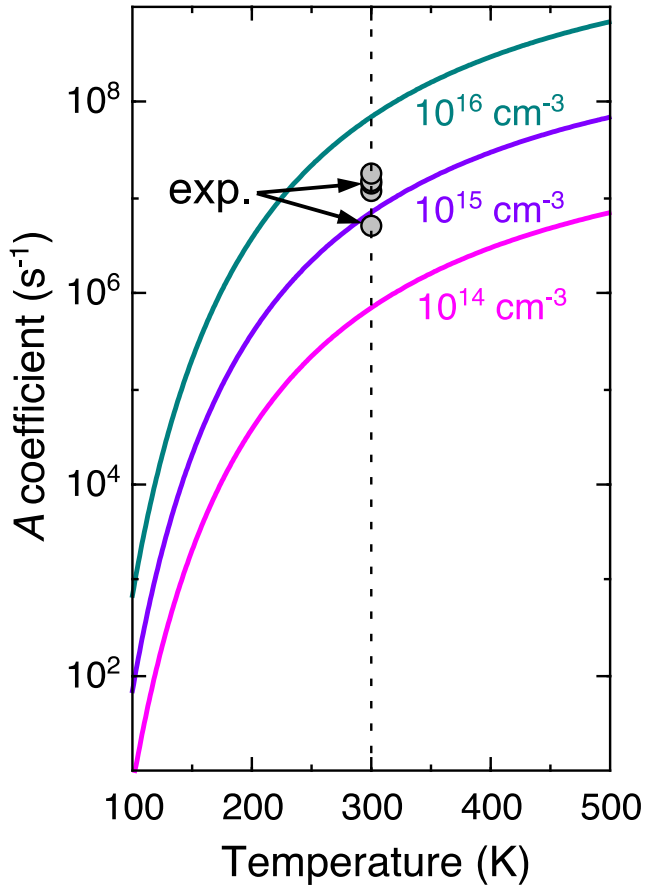

- Total capture coefficient:

$$C_{\text{tot}} = \frac{C_n^0 + C_p^0}{1 + \frac{C_n^0}{C_p^-} + \frac{C_p^0}{C_n^+}}$$

- Nonradiative recombination rate:

$$R = An \; ; \; A = N_{\text{def}} \, C_{\text{tot}}$$

- The iodine interstitial is an efficient nonradiative recombination center
- Likely responsible for the observed rates in experiments
  - $N_{\text{def}} \sim 10^{15}$ cm^{-3}
  - A. Baumann *et al.*, J. Phys. Chem. Lett. **6**, 2350 (2015); S. Heo *et al.*, Energy Environ. Sci. **10**, 1128 (2017).

$\Rightarrow A \approx 10^7$ s^{-1}

X. Zhang *et al.*, Phys. Rev. B **101**, 140101 (2020).

Other point defects

- Also examined other native point defects
- Pb interstitial (Pb_i) and antisites are high in energy
  $\Rightarrow$ unlikely to be present
- Iodine vacancy (V_I): no charge-state transition levels in the band gap $\Rightarrow$ cannot act as a recombination center
- Lead vacancy (V_{Pb}): explicit calculations of recombination rates show that V_{Pb} does not cause efficient nonradiative recombination

$\Rightarrow$ Iodine interstitial likely responsible for the observed nonradiative recombination: $A \approx 10^7$ s^{-1} for $N_{def} \sim 10^{15}$ cm^{-3}

- Iodine-rich synthesis conditions should be avoided
  - Extreme iodine-poor should be avoided as well
    - promote the formation of hydrogen vacancies

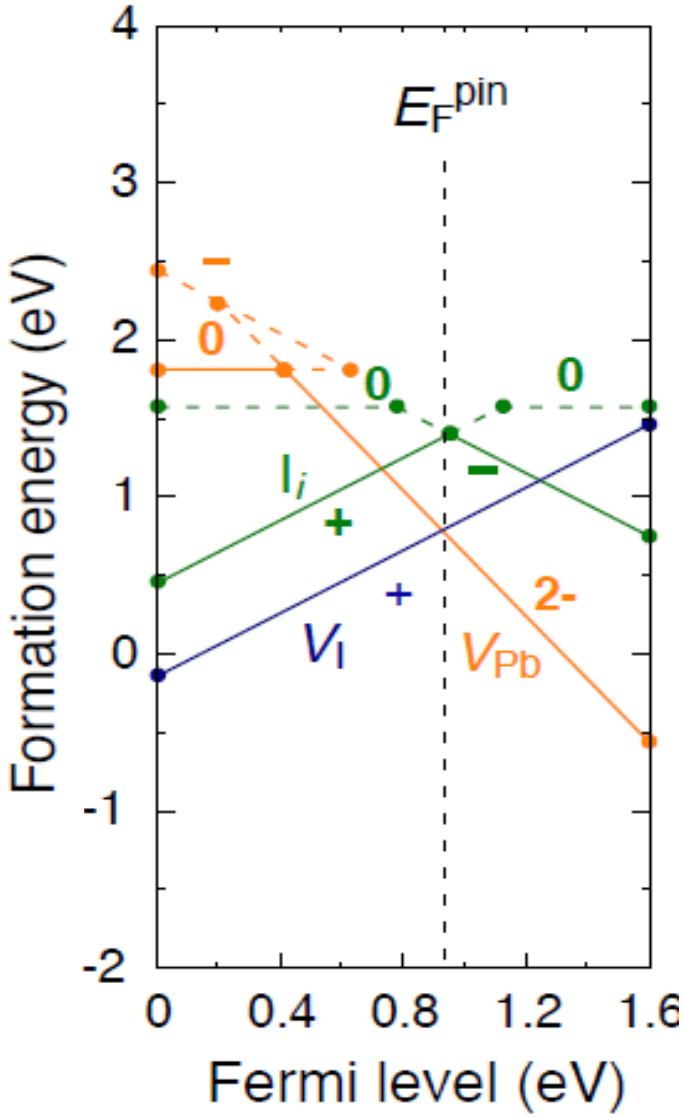

Hydrogen vacancies in $MAPbI_3$

- Hydrogen vacancies have been mostly overlooked when considering point defects
- MA: CH_3NH_3 → two types of H vacancies
  - V_H(C): removing H from a C atom
  - V_H(N): removing H from a N atom
- V_H(N) is an exceptionally strong recombination center (10^{-4} cm^3s^{-1})
- Present in high concentrations under I-poor and H-poor conditions

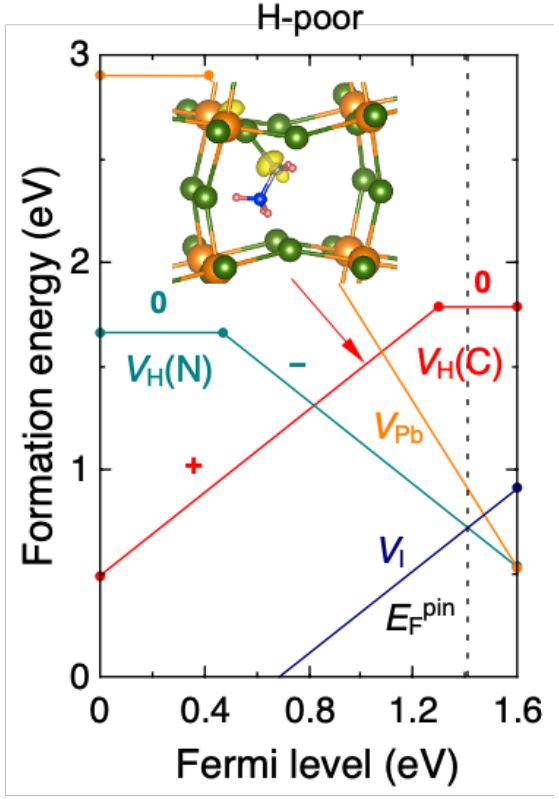

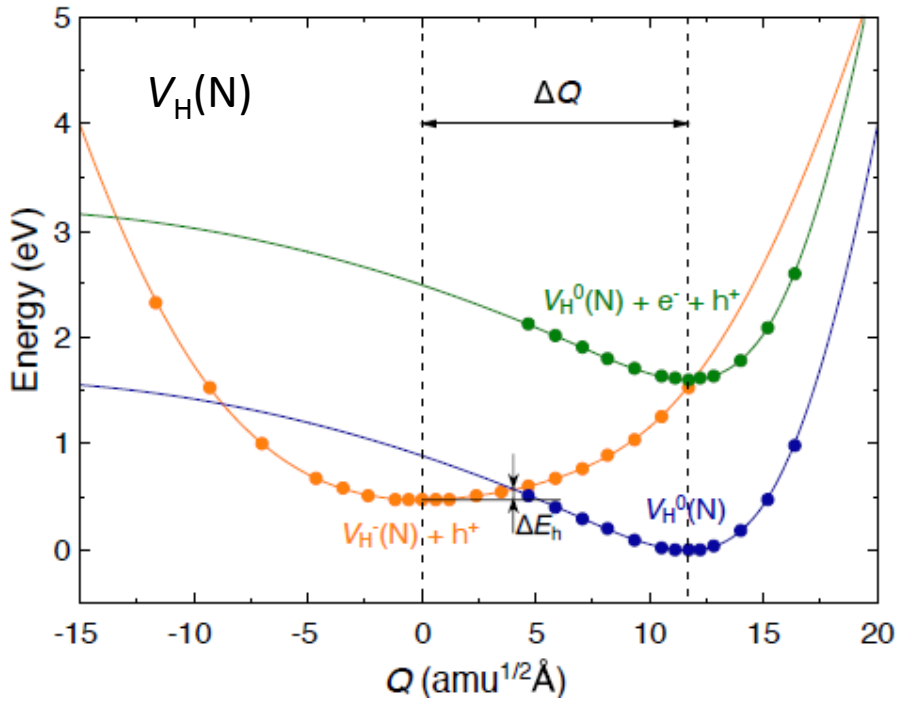

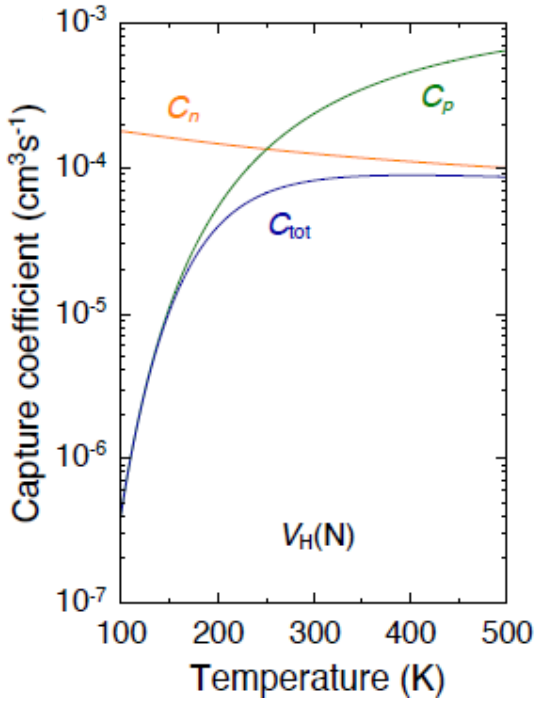

X. Zhang *et al.*, Nat. Mater. **20**, 971 (2021).

Qualitatively different behavior in $FAPbI_3$

- FA (formamidinium): $CH(NH_2)_2$
- V_H(C) and V_H(N) have much higher formation energies (lower concentrations) than in $MAPbI_3$
- V_H(C) has substantially lower capture coefficient
- Rationalizes why FA is essential for realizing high efficiency

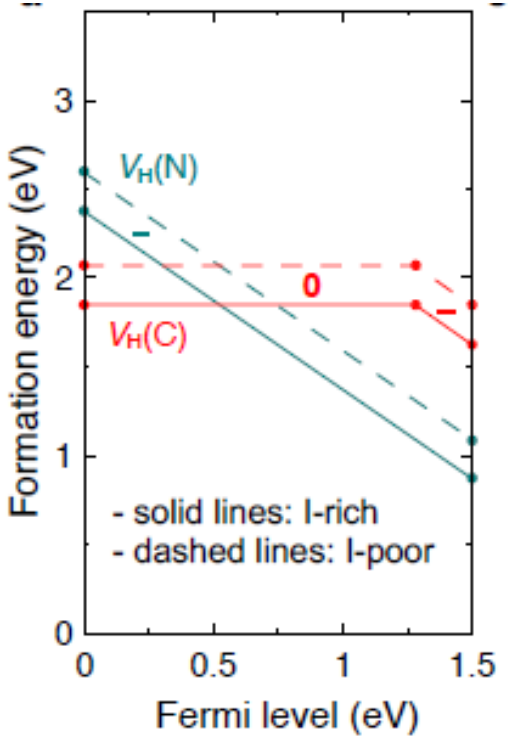

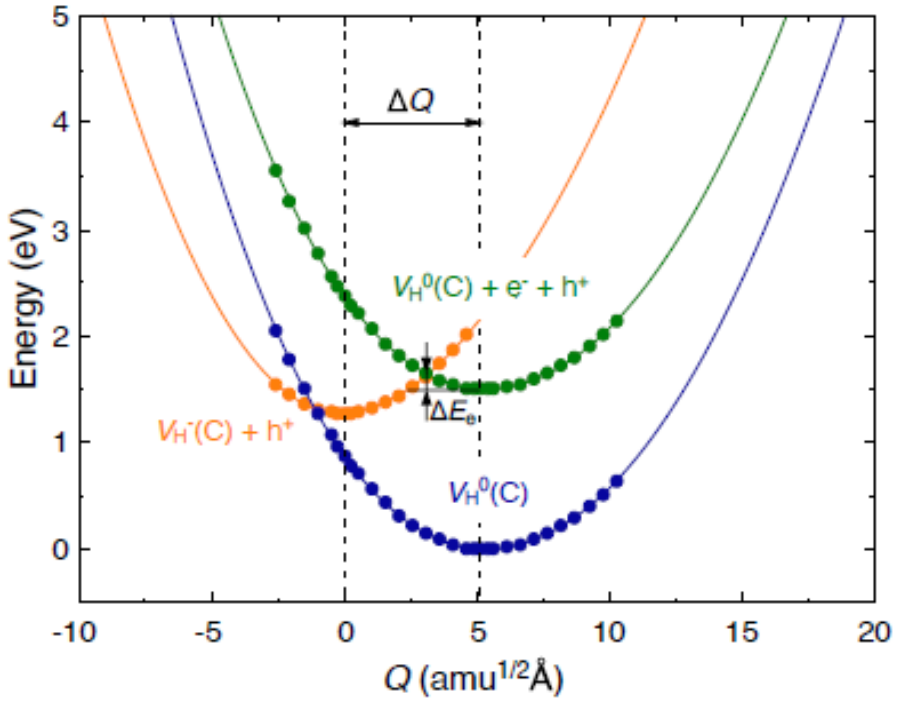

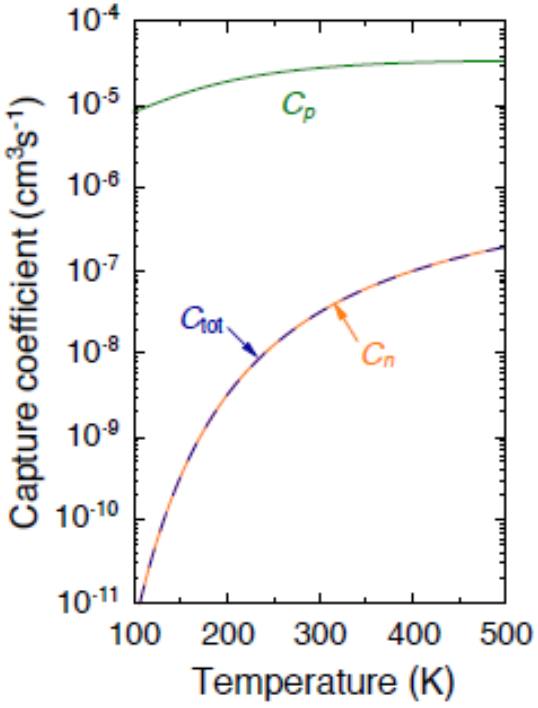

X. Zhang *et al.*, Nat. Mater. **20**, 971 (2021).

Getting rid of H vacancy problem by using $CsPbI_3$

- $CsPbI_3$: deep-level defects are present (V_{Pb}, I_{Cs}, and I_i)
- Explicit computation of recombination coefficients: I_i is the dominant recombination center
- Similar total capture coefficient as I_i in $MAPbI_3$, but no need to worry about H vacancies!
- Origin of current inferior performance of $CsPbI_3$: poor stability (small Cs^+ → small tolerance factor)
- Ways to enhance stability: alloying, strain, and improved growth techniques

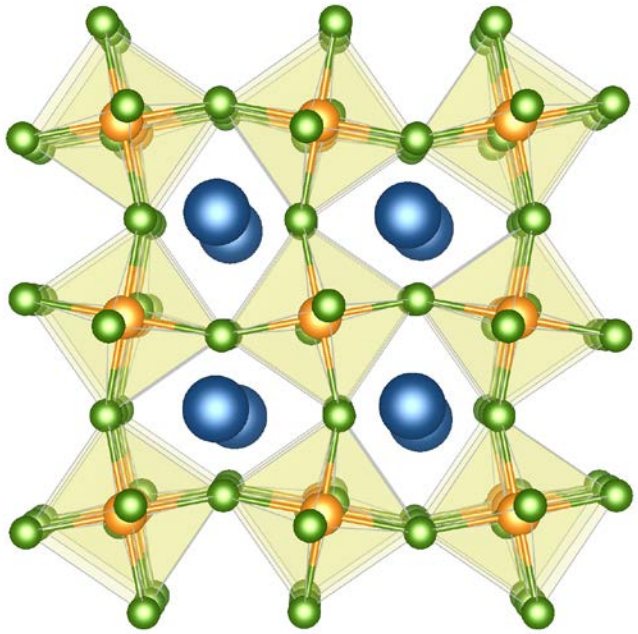

$CsPbI_3$

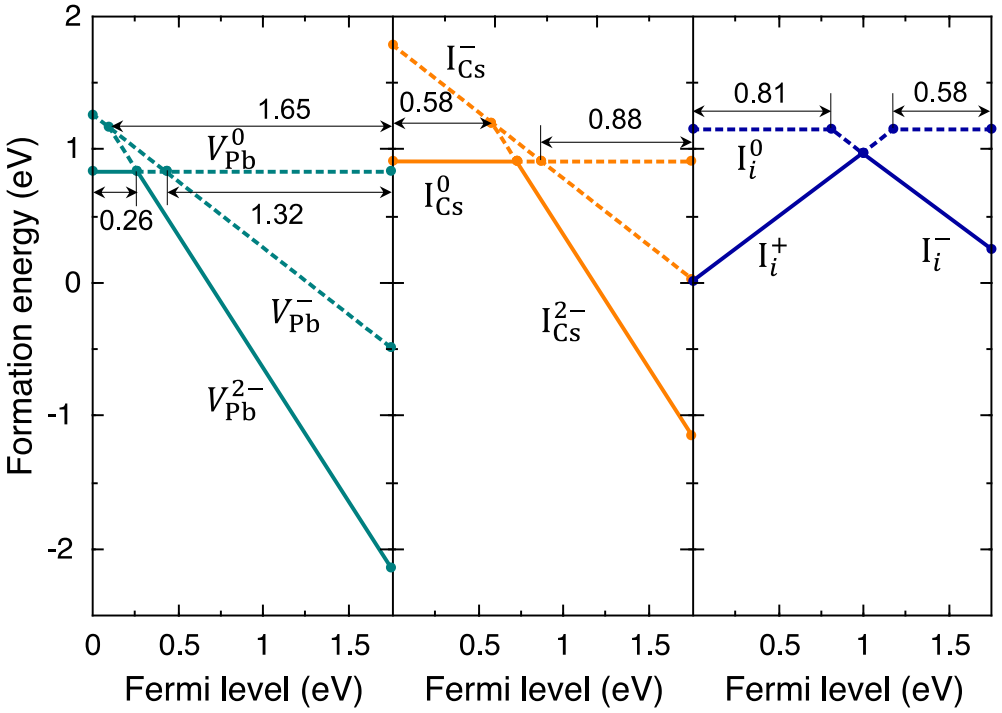

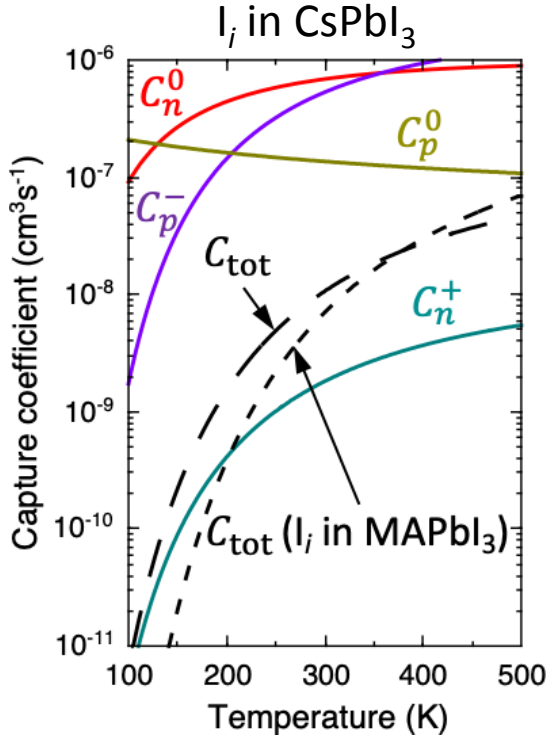

X. Zhang *et al.*, Cell Rep. Phys. Sci. **2**, 100604 (2021).

Putting values in perspective

- A coefficient in halide perovskites is comparable to or higher than those in conventional semiconductors
- Halide perovskites are often called "defect tolerant"
  - "Defects may be present, but do not harm efficiency"
  - Notion based on older calculations showing that defects do not introduce deep levels in the band gap
- Calling hybrid perovskites "defect tolerant" is misleading
  - We do not call GaAs or GaN "defect tolerant" —we worry a great deal about defects!
- Distinctive feature of hybrid perovskites: they can be grown with low defect densities using low-cost deposition techniques

Material	A coefficient (s^{-1})
$MAPbI_3$	1.4×10^7
$MAPbI_3$	1.5×10^7
$MAPbI_{3-x}Cl_x$	0.5×10^7
$MAPbI_{3-x}Cl_x$	1.2×10^7
$FAPbI_3$	0.7×10^7
$FAPbBr_3$	2.1×10^7
GaN	$0.1 – 1.0 \times 10^7$
GaAs	$0.05 – 0.4 \times 10^7$

M. B. Johnston *et al.*, Acc. Chem. Res. **49**, 146 (2016).
F. Olivier *et al.*, Appl. Phys. Lett. **111**, 022104 (2017).
E. Yablonovitch *et al.,* Appl. Phys. Lett. **50**, 1197 (1987).

X. Zhang *et al.*, J. Phys. Chem. C **124**, 6022 (2020).

Summary

- Rigorous first-principles calculations elucidate mechanisms
- Radiative recombination
  - Rashba spin splitting: spin texture, normal optical transitions
  - Rashba momentum splitting: limited impact, a factor of 2

    J. Phys. Chem. Lett. **9**, 2903 (2018); ACS Energy Lett. **3**, 2329 (2018).
- Auger recombination
  - Resonance in band structure
  - Band-structure and lattice-distortion engineering allows reducing Auger

    Adv. Energy Mater. **8**, 1801027 (2018); Adv. Energy Mater. **9**, 1902830 (2019).
- Defect-assisted SRH recombination
  - Halide perovskites often touted as “defect tolerant”; our work demonstrates that defects do impact efficiency.
  - Hydrogen-related defects act as strong nonradiative recombination centers

    X. Zhang *et al*., Phys. Rev. B **101**, 140101 (2020);
    J. Phys. Chem. C 124, 6022 (2020); Nat. Mater. 20, 971 (2021).